Solar Energy 170 (2018) 520–540

Contents lists available at ScienceDirect

Solar Energy

journal homepage: www.elsevier.com/locate/solener

Review

Concentrated solar energy applications in materials science and metallurgy

Daniel Fernández-González[a,*], I. Ruiz-Bustinza[b], Carmen González-Gasca[c], Juan Piñuela Noval[a], Javier Mochón-Castaños[a], José Sancho-Gorostiaga[a], Luis Felipe Verdeja[a]

[a] Grupo de Investigación en Siderurgia, Metalurgia y Materiales, Escuela de Minas, Energía y Materiales, Universidad de Oviedo, Oviedo, Asturias, Spain
[b] ETSI Minas y Energia UPM Madrid, Spain
[c] Universidad Europea – Laureate International Universities, Villaviciosa de Odón, Madrid, Spain

ARTICLE INFO

Keywords:
Concentrated solar energy
Metallurgy
Materials science
Ceramics
Materials processing
Fullerenes
Carbon nanotubes
Lime

ABSTRACT

New energy sources have been researched with the objective of achieving a reduction in the emissions of greenhouse gases as well as other polluting gases. Solar energy is one of the options as when properly concentrated offers a great potential in high temperature applications. This paper offers a review on all fields connected with materials where concentrated solar energy has been applied. These applications include metallurgy, materials processing (welding and cladding; surface treatments; coatings and surface hardening; and, powder metallurgy), and non-metallic materials (ceramics, fullerenes, carbon nanotubes, and production of lime).

1. Introduction

Energy consumption is one of the progress and welfare of societies measurements, and for that reason when there are problems with the energy sources (exhaust, wars, market changes, etc.), then there is an energy problem or energy crisis (for instance, oil crisis in 1973 and 1979, Venn, 2002). In this way, the search for new energy sources and the efficient use of the energy are in the research policies of the countries, especially of the developed countries. These policies form part of the idea of green economy that is rooted in the new industrial policies, with the objective of giving a quality brand to the industries of the developed countries, but also with the purpose of protecting nature and safeguard the health and quality of life of people that live in these countries.

Renewable energies include natural energy sources virtually inexhaustible, either because of being available in huge quantities or being able of regenerating by natural processes. According to this definition, renewable energy includes: biofuels, biomass, geothermal, hydropower, solar energy, tidal power, wave power and wind power. Solar energy is one of the most promising renewable energies as the temperatures that are possible to reach when solar energy is properly concentrated allows melting even ceramic materials, and in this way the number of applications in materials science and metallurgy are almost infinite. However, nowadays, the interest of solar energy is mainly focused on the field of energy, both thermal and electric, except for several research projects where the possible applications of solar energy in materials science are explored. The problem observed in most of these researches connected with materials science is the lack of continuity (not in all of them but is the general keynote), meaning that a certain field is explored and then abandoned, without an attempt of scaling up to pilot plant or industrial scale (searching for a commercial application). The reason for abandoning the topic maybe is the lack of interest by the industrial companies (generally solar processes are competitive in quality, time and temperatures with traditional methods in a laboratory scale but they are not industrially proved, and apart from that, these traditional methods are well known and currently installed in competitive plants) or the lack of promising results (but this question was not observed, in general). In fact, only few projects were scaled from laboratory to pilot scale, and none of them is commercially used in an industrial scale. Moreover, other factors that could limit the possible applications of solar energy in materials science and metallurgy are the uncertainty of sun availability (there are several places that offer an average yearly number of sun hours and sun radiation levels, but they cannot ensure daily weather conditions) or the location of the sun better conditions far from the industrial and populated regions. All above mentioned (and other questions that will be mentioned throughout the paper) could limit the possible applications of concentrated solar energy to materials recently discovered (as could be the case of fullerenes or carbon nanotubes), high added value processes and materials (that could compete with conventional methods) or fields

* Corresponding author at: Calle Independencia, 13, 33004, Oviedo, Asturias, Spain.
E-mail address: fernandezgdaniel@uniovi.es (D. Fernández-González).

https://doi.org/10.1016/j.solener.2018.05.065
Received 7 February 2018; Received in revised form 15 May 2018; Accepted 18 May 2018
Available online 05 June 2018
0038-092X/

Table 1
Parameters defining the operation of each technology (laser, plasma, and concentrated solar energy) (Flamant et al., 1999).

Technology	Typical power (kW)	Flux density (W/cm^2)	Surface area (cm^2)	Temperature (K)	Overall efficiency (%)	Capital cost (kECU/kW)
Laser					≃2	50–100 (1–5 kW)
CO_2	2–5	10^3 to 10^6	< 1	> 5000		
Nd-YAG	≃0.5	10^5 to 10^9 (pulsed)	< 1	> 5000		
Plasma	10–2000	10^4	≃100	> 5000	25	0.8–1.5 (50–1000 kW)
Solar Furnace	≤1000	10^3	≃1000	≤3500	60	1.2–1.8 (50–1000 kW)

where new high energy technologies such as laser or plasma are applied. In Table 1, it is possible to find the parameters that define each technology (laser, plasma, and concentrated solar energy) according to Flamant et al. (1999).

According to Flamant et al. (1999) capital costs and efficiency could be competitive for concentrated solar energy if compared with laser and plasma technologies. However, the couple concentrated solar energy-materials is still an immature technology being this question responsible of the appearance of many different applications in different fields. In order to have a wide view of the possibilities of concentrated solar energy, we will try to collect most of those connected with materials science, metallurgy, and ceramics. As we will see, the couple metallurgy-energy for the ZnO/Zn seems to be the most developed and interesting technology, as this field is the most prolific regarding the number of research projects, but also regarding the scaling up to pilot plant.

First of all, we will try to find the origins of the solar energy application in the field of materials science. It should be considered that modern solar furnaces and solar installations were most of them built in the late seventies or early eighties in a context of energy crisis (1973 and 1979 oil crisis). It should be also considered that solar furnaces and solar installations were originally built with the purpose of searching for new energy sources in a context of high oil prices. There were several previous solar installations, being the most important that proposed by Felix Trombe and built after the Second World War in France. Felix Trombe, Marc Foex and Charlotte Henry La Blanchetais restarted the researches of Lavoisier in the 1946–1949 in Meudon (France) by building a parabolic concentrator of 2 kW used in chemistry and metallurgy at high temperatures, and after that, the 50 kW solar furnace of Mont Sant Louis was built in 1949. However, most of the solar installations were built after the first energy crisis: *PSA, Plataforma Solar de Almería* (early 80 s, 60 kW solar furnace and 3360–7000 kW solar tower, Herranz and Rodríguez, 2010), research is mainly connected with energy issues in this installation; CENIM-CSIC and UCLM (from 90 s, 0.6 kW Fresnel lens equipment, Herranz and Rodríguez, 2010); *PROMES (Procédés, Materiaux et Énergie Solaire, CNRS)* is the main research center that explores the couple concentrated solar energy-materials, which has its early origins in Mont Louis, but being the solar furnaces of Odeillo (final 60 s, different furnaces 0.9 kW, 1.5 kW, 6 kW and 1000 kW (see Fig. 1 and Fig. 2), Herranz and Rodríguez, 2010) the current installation; *Solar furnace of Uzbekistan* (built in 1981, 1000 kW); *High flux solar furnace at DLR (German Aerospace Center)* in Cologne-Porz (1994, power up to 22 kW, Herranz and Rodríguez, 2010), significant experience on testing materials; *Solar Technology Laboratory* at the *Paul Scherrer Institute (PSI)*, stablished in 1988 in Villigen (Switzerland), they offer the High-Flux Solar Furnace (1997, 40 kW), 300 kW solar pilot plant (commissioned in 2005, EU project SOLZINC) to perform the carbothermal reduction of zinc oxide, and 100 kW solar pilot plant (commissioned in 2011, BFE project Solar2Zinc) for the thermal dissociation of zinc oxide to produce zinc and syngas; *Weizmann Institute of Science* of Israel (3000 kW solar tower, from the late 80 s; 50 kW solar furnace from the early 80 s); *National Solar Thermal Test Facility (NSTTF)* operated by Sandia National Laboratories for the U. S. Department of Energy (1979, 16 kW solar furnace, Herranz and Rodríguez, 2010); *National Renewable Energy Laboratory (NREL)* (1977), have a high-flux solar furnace of 10 kW in

Fig. 1. Medium size solar furnace at Odeillo (1.5 kW foreground, 0.9 kW background).

Fig. 2. 1000 kW solar furnace of Odeillo.

operation since 1990 in Golden (Colorado); *Korea Institute of Energy Research (KIER)*, (21st century, 40 kW solar furnace; 10 kW disc type solar concentrator), mainly dedicated to solar applications in the field of energy (Konstandopoulos et al., 2012); and, *Commonwealth Scientific and Industrial Research Organization (CSIRO)*, (21st century, 500 kW solar tower) also mainly devoted to solar applications in the energy field (Konstandopoulos et al., 2012).

Historically, the first use of concentrated solar energy in the transformation of materials is found in the Roman's period. During the Siege of Syracuse (Second Punic War, 215 before JC) the legend tells that Archimedes used mirrors to destroy the Roman naval fleet composed of wooden ships (Rossi 2010). However, the first real and most important application of solar energy in materials processing is the sun drying of adobe bricks, low temperature sun process applied since at least 10,000 years (Revuelta-Acosta et al., 2010; Rodríguez and Soroza, 2006). In this line, Martínez et al. (2015) studied the applications of

high temperature solar energy in construction ceramics manufacturing industrial process by using a brand-new device at a solar furnace (PSA) for proof-of-concept testing. In this way, they improved the knowledge on how to deal with these high temperature processes and identified several problems as the lack of uniformity on the thermal treatment and the obtaining of achievable heating and cooling rates. The utilization of concentrated solar energy in construction ceramics could reduce energy costs, and in this way, could both improve the quality and reduce the costs of construction materials in some regions with good irradiation conditions. The first investigations regarding the possible applications of concentrated solar energy date from the 17th century, a mathematician from Germany, Ehrenfried Walter Von Tschirnhaus designed, constructed and worked with lenses and mirrors with the objective of concentrating solar energy (Gosh, 1991; Newcomb, 2009; McDonald and Hunt, 1982), he melted iron and obtained ceramics (porcelain) with solar energy (Gosh, 1991; Newcomb, 2009; McDonald and Hunt, 1982). Other researchers worked with concentrated solar energy during the Modern Period: Cassini (17th century) designed a lens with 1 m in diameter to reach temperatures of around 1000 °C, and he melted iron and silver with it; Lavoisier (18th century) melted iron and approached the melting point of platinum (Flamant and Balat-Pichelin, 2010). Lavoisier also showed that it was possible to treat metals under special atmosphere like nitrogen (Flamant and Balat-Pichelin, 2010). Felix Trombe demonstrated how to use solar energy with the purpose of melting high melting point refractory ceramics (alumina, chromium oxide, zirconia, hafnia and toria) after the Second World War (Flamant and Balat-Pichelin, 2010). In the same period, Tetsuo et al. (1957) and Tetsuo et al. (1959) studied the melting of several metal oxides. The growth of crystals of high temperature materials (from simulated lunar materials) studied by Farber (1964) is also from the same period.

The first industrial applications of concentrated solar energy in the field of materials were focused on studying the behavior of materials under high temperature conditions (for instance, space plane Hermes had its thermal protection system tested in the Plataforma Solar de Almería in the early 90 s (Martínez and Rodríguez, 1998; Van den Abeelen 2017)). Other researches in the line of studying the behavior of certain materials under extreme conditions are: D'Elia et al. (2014) characterized SiC based micro-concrete used in nozzles for space applications in a 2 kW solar furnace under high temperature oxidation conditions; Charpentier et al. (2011) studied the physical, chemical, and intrinsic properties of refractory materials treated with concentrated solar energy in a real environment; Kovacik et al. (2014) studied the thermal shock behavior of 37MnSi5 steel coated with TiB_2 ceramic by using a 5 kW vertical solar furnace at PSA. Apart from studying the behavior of materials under high temperature and extreme conditions, the research for new uses of concentrated solar energy in processes and treatments of materials has reached great interest, particularly in Europe, with alliances (Sollab, Alliance of European Laboratories for Research and Technology on Solar Concentrating Systems, 2004) and European research programs (SFERA, Solar Facilities for the European Research Area, 2009–2017)). The interest in concentrated solar energy has also reached other countries, Eglinton et al. (2013) studied the potential applications of concentrated solar energy in Australian minerals processing and extractive metallurgical industries, due to the sun availability in Australia, the importance of mining and metallurgical industries in this country, and the high temperatures that is possible to reach by using concentrated solar energy.

This paper will try to summarize the applications of concentrated solar energy in the field of materials (production and processing) with the idea of offering a reference for the researchers and industrials that could be interested in using concentrated solar energy in materials and metallurgical processes.

2. Solar energy applications in metallurgy

2.1. Silicon

Silicon is a material widely used, especially in: electronics, metallurgy (alloys), and photovoltaics. The production of silicon is nowadays carried out through carbothermal reduction of silica in electric furnaces. Several qualities of silicon are produced depending on the above mentioned applications: *electronic-grade* of high purity (99.99999% Si), produced through an expensive process as a consequence of being energy and resource intensive; *metallurgical-grade* (99% Si), used as raw material for electronic-grade silicon production; and, *solar-grade*, with quality intermediate to the other two. Murray et al. (2006) proposed a two-step process to produce solar-grade silicon. The first step is based on the production of silicon nitride (Si_3N_4) through carbothermal reduction of SiO_2 in nitrogen atmosphere at temperatures below 1500 °C for more than 4 h. The reaction that governs the first step of the process proposed by Murray et al. (2006) is:

$$3SiO_2 + 6C + 2N_2 = Si_3N_4 + 6CO$$

The second step is based on that if the kinetics of recombination of $Si(l)$ with $N_2(g)$ is slow enough it is possible to dissociate the nitride to produce silicon. The purification is performed with reactive gas such as H_2, N_2 and O_2 or vacuum to remove boron and phosphorous.

The advantages of the process proposed by Murray et al. (2006) can be summarized as follows: the impurities that the carbon electrodes of the conventional high-temperature arc process produce in the silicon are eliminated by using concentrated solar energy; costs could be significantly reduced (concentrated solar energy costs are not dependent on the temperature, in conventional process, the higher the temperature the higher the energy requirements; but installation costs could be higher than in conventional process); and, CO_2, NO_x and SO_x emissions are reduced as combustibles used in heating are not used in the process proposed by Murray et al. (2006).

The manufacture of silicon under vacuum ($3{\cdot}10^{-3}$ bar) and temperatures in the range 1997–2263 K through solar carbothermal reduction of SiO_2 was studied by Loutzenhiser et al. (2010). The formation of Si(g) is expected at lower temperatures when reducing the total pressure in the carbothermal reduction of SiO_2. They carried out the experiments at the Paul Scherrer Institute High Flux Solar Simulator with mixtures of charcoal and silica. Flux intensities equivalent to 6500 suns allowed for reaching Si purities ranging from 66.1 to 79.2 wt%, with Si purity increasing with the temperature. This process, the same as that proposed by Murray et al. (2006), could be interesting since the environmental and energy costs point of view, although reaching vacuum conditions requires energy consumption (and this would mean costs). The problem is that Si purities are very low (< 80%) if compared with the Si purities that is possible to attain in the current industrial process (> 99%). This question indicates that the process should be significantly improved to be used in the production of metallurgical grade, solar grade or even electronic grade silicon. In the event of obtaining Si purities > 99%, the solar process could be competitive because silicon production is energy intensive.

The purification of metallurgical-grade silicon was other of the processes performed by using concentrated solar energy and concerning silicon. Flamant et al. (2006) performed experiments in a vertical axis solar furnace in Odeillo with the purpose of removing boron and phosphorus by vaporization. They treated upgraded metallurgical silicon provided by RIMA (5.7 ± 1.4 ppm B and 9.4 ± 2.4 ppm P) under 0.05 atm to favor P vaporization, using $1l/min$Ar + 2.5 mlH_2O to favor B vaporization as BOH, at temperatures within 1550 °C and 1700 °C. Flamant et al. (2006) observed an efficient removal of B and P after 50 min treatment (3.2 ± 0.8 ppm P, 2.1 ± 0.5 ppm B). However, the efficient results were only achieved for phosphorous removal according to the solar grade silicon requirements (< 5 ppm P, < 1 ppm B), but

more studies in this line could be very useful to treat to remove both boron and phosphorus, and not only phosphorus.

2.2. Aluminum

Aluminum production is an energy-intensive process independently of the technology used, being the Halt-Hérault's process the main technology used in the aluminum production (Sancho et al., 2000). Other alternative processes are: *ALCOA process*, which is based on the electrolysis of $AlCl_3$ in LiCl-NaCl salts bath at 700 °C by using non-consumable electrodes of graphite; *aluminum nitride electrolysis*; *aluminum sulphide electrolysis*; *ALCAN process*; and, *direct reduction of alumina;* but none of these alternative processes can compete with the Halt-Hérault's process. Murray (1999a) proposed concentrated solar energy as energy source from a conceptual point of view in the production of aluminum. Murray (1999a) considered two processes: direct reduction process to Al or Al-Si alloy, and reduction process to an intermediate product such as AlN or Al_2S_3 that could be more easily electrolyzed than Al_2O_3 without using consumable electrodes. As it is possible to see processes proposed by Murray (1999a) are based in the alternative process to the Halt-Héraut process.

Carbothermal reduction of aluminum and silicon oxides is a technical challenge because of the temperature required (2100–2300 °C) but could be solved by means of concentrated solar energy (Murray, 1999b, 2001). Murray (1999b) and (2001) used a black-body cavity receiver placed at the focus of the Paul Scherrer Institute's 70 kW tracking parabolic concentrator, and he found a small amount 61/37 wt % Al/Si alloy formed, and the partially reacted pellets showed conversion to Al_4C_3 and SiC. Murray (2001) also carried out experiments in Odeillo 2 kW solar furnace, where he observed both aluminum by direct carbothermal reduction and Al-Si alloy via carbothermal reduction of a mixture of alumina, silica and carbon. This process could be very useful because Al-Si alloy could be directly obtained in a single step, although conversion to Al_4C_3 and SiC was observed, and the presence of these phases reduces the quality of the obtained alloy. If the process would be improved to avoid these phases, reduction in energy costs (with respect to the Halt-Hérault process) as well as reduction in contamination coming from the anodes could be achieved. However, continuity is not observed, and the potential impact of this application of concentrated solar energy is not checked.

Aluminum production is energy-intensive process as we mentioned (17.4 kW/kg of electrical energy for an older plant (Murray 1999b)). Lytvynenko (2013) described the obtaining of aluminum by electrolysis through the Hall-Herault's process without using electric power, by using solar energy. Cell heating is produced through a concentrator of solar radiation, while electrolysis process is carried out by direct electric current from a solar battery. The initial mixture contained alumina powders (Al_2O_3) and cryolite (Na_3AlF_6) in a ratio 1:9 with total weight of 15 g. The process proposed by Lytvynenko (2013) is a version of the Halt-Hérault process but using solar energy as energy source in all steps. Even when this version has a strong potential in the aluminum industry as energy costs would be significantly reduced (around 40% of the costs of producing aluminum belong to energy costs), and thus the costs of producing aluminum would be significantly reduced. However, and as we will see later, the quantities of aluminum produced through this via should be significantly increased to compete with the traditional Halt-Hérault process.

The solar aluminum production under vacuum conditions was also studied. Kruesi et al. (2011) studied the aluminum production through vacuum carbothermal reduction of alumina at the Paul Scherrer Institute, and they observed that under vacuum conditions, the production of aluminum is facilitated by lowering the onset temperature for this reaction and by shifting the formation of free Al (g) to a temperature range where it is thermodynamically unfavorable the formation of Al_2O, Al_4C_3 and Al-oxycarbides. Kruesi et al. (2011) observed that under Ar atmosphere at 3.5 to 12 mbar total pressure, Al and CO were formed in the gas phase from alumina and charcoal at 1387 °C accompanied by Al_4C_3 and Al_4O_4C. Vishnevetsky et al. (2013) studied the solar carboreduction of alumina under vacuum conditions, and observed alumina to aluminum conversion about 90% for reaction at above minimum temperatures, while at lower temperatures a significant amount of solid Al_4C_3, Al_4CO_4 and volatile Al_2O appeared. Vishnevetsky and Epstein (2015) studied the solar carbothermal reduction of alumina (Al_2O_3), magnesia (MgO) and boria (B_2O_3) under vacuum conditions. They prepared stoichiometric mixtures with beech wood charcoal as biomass source, oxide powders and 10 wt% sugar powder (as binder). Mixtures were pressed at 10 tons to obtain pellets, which were baked at 165 °C for 20 min in an oven. Experiments were carried out in a vacuum reactor at one of the Weizmann Institute of Science's solar facilities. Vishnevetsky and Epstein (2015) observed that almost all alumina reacted, with presence of carbides and oxycarbides formed during preheating. They also observed residual unreacted magnesia probably due to large magnesia particles and their possible sintering at high temperature (Vishnevetsky and Epstein, 2015). Fast boron carbide (decompose only above 2000 °C) formation before reaching reduction temperatures in the reaction zone difficulties the carboreduction of boria, being boron carbide the main product (Vishnevetsky and Epstein, 2015). In these cases, the utilization of vacuum atmosphere would reduce the operation temperatures, but the appearance of carbides, oxides and oxycarbides could reduce the quality of the product obtained.

Even when the production of aluminum is energy intensive, and the development of technologies that could reduce the energy consumptions would led to improvements in competitiveness of the aluminum industry, the processes described in this section do not seem reasonable considering the amounts of aluminum produced nowadays in industrial plants. An electrolytic cell in the aluminum industry can produce $1.2–1.5 \cdot 10^6$ g of aluminum daily (approximately, it depends on the plant and operation requirements and conditions), around 5 orders of magnitude more than that produced through the proposed method based on concentrated solar energy (authors mention quantities of grams). It does not seem reasonable, for that reason, producing nowadays aluminum through concentrated solar energy via. The same reasoning could be applied in the case of the silicon. The difference between the aluminum and the silicon situations, is that in the case of the aluminum, it is produced in important quantities with suitable quality for its typical applications, while in the case of the silicon, the electronic grade silicon as high purity material produced in not large quantities could be obtained through concentrated solar energy if the process is significantly improved in quality (for instance, the Si purity obtained by Loutzenhiser et al. (2010) is far from that required even for the silicon of metallurgical grade) and in quantity (at least several tens of kilograms daily).

2.3. Zinc

The same as in the case of the aluminum and the silicon, zinc plants produce huge amounts of zinc (for instance that located in San Juan de Nieva (Avilés, Asturias, Spain) belonging to Asturiana de Zinc (Glencore) produced 517,962 tons of zinc in 2016). These quantities seem unattainable for any process based on concentrated solar energy (nowadays). However, and as opposed to the cases of the aluminum and the silicon, the couple Zn-solar energy has a great potential in the field of energy storage (as zinc can be used in water and carbon dioxide splitting). First researches date from the eighties when Fletcher and other researchers investigated the reduction of ZnO to Zn by means of concentrated solar energy (Fletcher and Noring, 1983; Fletcher et al., 1985; Palumbo and Fletcher, 1988). More modern research works as that of Hauter et al. (1999) proposed the thermal dissociation of ZnO into zinc and oxygen at above 2000 K.

Osinga et al. (2004a) studied the carbothermal reduction of ZnO with solid carbon as reducing reagent in a 5–10 kW solar furnace. The

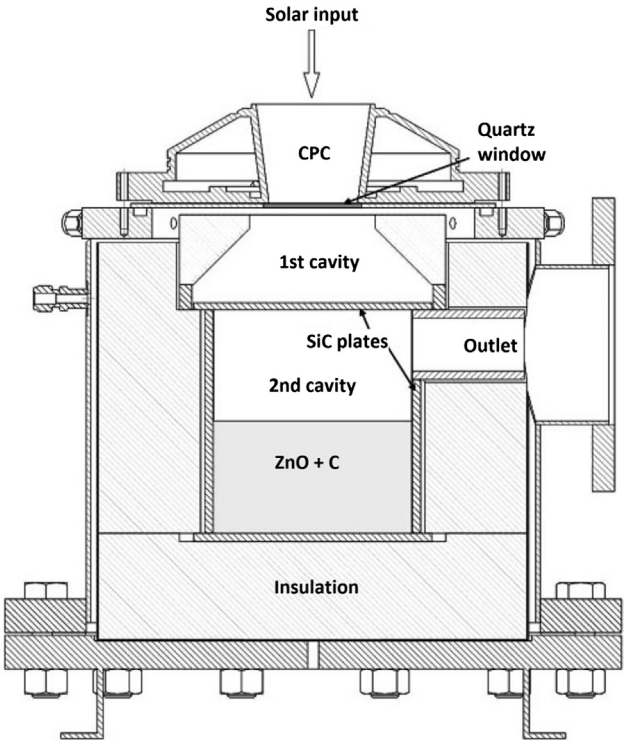

Fig. 3. Solar chemical reactor configuration for the carbothermic reduction of ZnO with two cavities in series (1st as solar absorber and 2nd as reaction chamber) (reprinted from Osinga et al. (2004b). Copyright 2004 American Chemical Society).

solar reactor (which operated under vacuum pressure of 5–10 mbar) that they used had two chambers in series with one that acted as solar absorber (external) and the other as reaction chamber (internal) (Fig. 3). Produced gases were extracted from the reaction chamber by a N_2 flow, and then, after leaving the reactor, the products passed through a water cooled Pyrex tube where part of the zinc condensed (the remaining products were collected by a filter). Experiments lasted between 30 and 75 min, including 20–30 min of heating and reaching stationary conditions. Graphite absorber (solar absorber) reached 1500–1700 K while reagent's temperature was in the range 1350–1550 K. Osinga et al. (2004a) loaded mixtures of 500 g (C/ZnO molar ratio of 0.8/1) of ZnO powder and as reducing reagents carbon powder, beech charcoal powder and petroleum coke (Adinberg and Epstein, 2004 studied the carbothermal reduction of zinc with graphite; Steinfeld et al. (1998) used natural gas (CH_4) as reducing reagent, achieving yields in the zinc reduction of 50% at temperatures of 1300 K and 90% at temperatures of 1500 K). Osinga et al. (2004a) observed that 80% of the Zn was found in the gaseous flow as metallic zinc and the 20% remaining diffuses towards the interior of the insulating material. Epstein et al. (2004) studied the ferro-reduction of ZnO in an attempt of solving the problems with lead in Zn precipitation. Different reactors have been proposed, see Table 2.

As it was previously mentioned, Zn reduction finds application in the energy industry. Zinc can be used in water splitting with the finality of producing H_2, but other option is using zinc as combustible in batteries and combustible cells. In this way, solar process would be used as a method of storing solar energy as chemical combustible, because zinc is fed as combustible to a cell with the purpose of producing electricity, and then, the ZnO that was produced in the cell is recycled in the solar furnace (Wieckert et al., 2004). Several plants were built or designed to scale-up the process to a pilot plant: Wieckert et al. (2006) (EU-SOLZINC, 0.3 MW, production of 50 kg Zn/h, 95% purity, 2.5–5 μm particle size, 2 chambers reactor), Epstein et al. (2008) (5 MW, conceptual design of demonstration plant, 1700 kg Zn/h; 30 MW, conceptual design of demonstration plant, 11,000 kg Zn/h), Schunk et al. (2009b) (rotating cavity-receiver, validated a 10 kW reactor prototype in a high-flux solar simulator; studied the scaling up to 1 MW solar thermal power input), and Villasmil et al. (2013) and Koepf et al. (2016) (100 kW pilot plant at the Paul Scherrer Institute).

Thermochemical production of solar fuels from CO_2 and H_2O could be carried out by using volatile oxides different from ZnO. In this line, Levêque and Abanades (2013) and Levêque and Abanades (2015) investigated the thermal and carbothermal reduction of ZnO, SnO_2, GeO_2 and MgO. The reduction of several alkali metal hydroxides (Na, K and Li with carbon) using concentrated solar energy at high temperatures (900–1600 °C) generates CO, H_2 and the alkali metal (Epstein et al., 2001), being then possible combusting the CO/H_2 mixture in a gas turbine to generate electricity. Chambon et al. (2011) investigated the high-temperature thermal dissociation of ZnO and SnO_2 in a lab-scale 1 kW solar reactor under reduced pressure. In the event of considering also the variable recycling, the Waelsz oxide could be used. Waelsz oxide is produced in electric arc furnaces as powder during the recycling of galvanized steels and contains 55–65% Zn as oxide (Tzouganatos et al., 2013). Tzouganatos et al. (2013) proposed a new method for the purification of Waelsz oxide and the production of zinc using concentrated solar energy. They clinkered Waelsz oxide and reduced it with carbon in a 10 kW_{th} packed-bed solar reactor, and achieved impurities below 0.1 wt% (when clinkering above 1265 °C) yielding 90% wt. Zn when using biocharcoal as reducing agent at 1170–1320 °C. The zinc produced through this via could be integrated in the process of water-splitting to produce H_2. The couple Zn-energy could be used in energy storage and thus solve the problem of producing electricity 24 h every day via solar energy.

2.4. Iron and manganese

Nowadays, steel is mainly produced in both integrated steel plants from iron ore and via blast furnace-converter-secondary metallurgy (> 60% world steel production), and electric furnaces (Sancho et al., 2000). However, there have been several attempts of using solar energy in the ironmaking and steelmaking industry but without any possibility of competing with current steel factories that operate 24 h 365 days each year producing millions of tons (the availability of solar energy throughout the day would limit the applications of solar energy in the ironmaking). Sintering, performed with the purpose of obtaining a suitable product to be loaded into the blast furnace, also handles amounts close to millions of tons yearly (Fernández-González et al., 2016, 2017a, 2017b, 2017c, 2017d). The researches mentioned below were focused on either basic knowledge of decomposition of iron oxides or the recovery of valuable by-products of the ironmaking and steelmaking. The recovery of iron as oxide from different metallurgical by-products could be the field where concentrated solar energy could find application, in plants which could handle several tens of tons daily. However, only the research carried out by Ruiz-Bustinza et al. (2013) with the objective of obtaining magnetite from mill scale was found in this field.

Sibieude et al. (1982) studied the influence of temperature, partial pressure of oxygen and quenching speed on the decomposition rate of magnetite. 300 °C above the melting point of the magnetite under air atmosphere, there is 40% decomposition while under argon atmosphere complete decomposition is reached. This research offers a basic, but useful, knowledge about magnetite decomposition under different atmospheres. This question may be useful in the treatment of high-Fe wastes, as iron could be transformed into magnetite through the method proposed by Ruiz-Bustinza et al. (2013) (iron could be collected from these wastes as magnetite through magnetic methods), and then transformed into iron through the method described by Sibieude et al. (1982). In this way, wastes from different metallurgical processes (slags, powders, muds, etc.) could be treated, and they would become in potential iron ores.

Table 2
Different reactors for zinc oxide reduction.

Packed bed reactors	Wieckert et al. (2006) (300 kW; carbothermic reduction of ZnO) Osinga et al. (2004b) (carbothermic reduction of ZnO at 400–1600 K) Schunk et al. (2009a) (Zinc dissociation)
Aerosol and entrained flows	Perkins et al. (2008) (Zinc dissociation; residence times, 1.11–1.78 s; conversions, 6–17%; temperatures, 1873–2023 K) Koepf et al. (2015) (ZnO powder and charcoal; conversions, 12.4%) Brkic et al. (2016) (downward flow ZnO and carbon particles; heated by an opaque intermediate solar absorption tube; fast heating rate; short residence times)
Rotary semi-batch designs	Abanades et al. (2007) (thermal reduction of metal oxides in water-splitting for hydrogen production) Hauter et al. (1999) (dissociation of ZnO into Zn and oxygen at > 2000 °C) Chambon et al. (2010) (dissociation of ZnO; yields up to 87%) Müller et al. (2006) (Zn with purity exceeding 95 mol%) Schunk et al. (2008) (ZnO dissociation)
Others	Koepf et al. (2012) (beam-down gravity-fed solar thermochemical reactor) Brkic 2017 (drop-tube reactor heated with concentrated solar radiation; vacuum carbothermic reduction of ZnO) Vishnevetsky et al. (2006) (solar reactor in which a SiC crucible replaces the window, being irradiated from top using a beam down optics)

2.4.1. Magnetite production

Ruiz-Bustinza et al. (2013) studied the treatment of mill scale (produced in the steelmaking process in amounts of 5 kg/ton steel; chemical composition: 75% FeO, 5% Fe_2O_3, 10% Fe and 10% other) by means of concentrated solar energy with the purpose of obtaining magnetite. The interest of magnetite is the feasibility of being easily concentrated because of its magnetic properties. They used a solar furnace of fluidized bed (750 °C for 4 h), heated with concentrated solar energy installed in the Plataforma Solar de Almería, where they loaded pre-oxidized to hematite (Fe_2O_3) mill scale pellets (see scheme in Fig. 4). The proposed method could be interesting to recover valuable components from a steelmaking waste such as the mill scale, and using it combined with the processes used to obtain direct reduction iron (Sancho et al., 2000). However, they only mention iron as the element to be recovered when the presence of other alloying elements such as tungsten, vanadium and molybdenum is typical in this waste, making interesting the treatment of mill scale in a separated process (different from the typical practice of mixing mill scale with the mixture to be sintered) to recover also them. Neither is also said about the presence of water and oil in the mill scale and the problems that could imply the presence of these elements.

2.4.2. Fe_2O_3 and MnO_2 treatment

Steinfeld and Fletcher (1991) stablished the basis of the Fe_2O_3 reduction in solar furnace in presence of graphite as reducing reagent, at temperatures between 1300 and 2390 K yielding Fe maximum contents of the 78%. Steinfeld et al. (1993) carried out experiments to study the coproduction of iron and synthesis gas by Fe_3O_4 reduction with methane. Mochón et al. (2014) studied the direct use of concentrated solar energy in the carbothermal reduction of iron oxides (Fe_2O_3) and manganese oxides (MnO_2). Tests were carried out in the vertical axis solar furnace at Odeillo and they observed partially reduced products (Fe_3O_4, FeO and MnO) in their attempt of obtaining iron by direct reduction and ferromanganese. Fernández-González et al. (2018) observed the thermal decomposition of Fe_2O_3 into Fe_3O_4 and FeO after treating mixtures of iron oxide (III) and carbon in a 1.5 kW solar furnace at Odeillo. Fernández et al. (2015) applied multivariate statistics and fuzzy logic models to the analysis of the variables involved in the process of treating iron oxides in a solar furnace considering the information obtained during the campaign of experiments described in Mochón et al. (2014). All researches in this group are focused on basic questions about reducing iron and manganese oxides by using concentrated solar energy. They observed that magnetite (Fe_3O_4) is easily obtained in all experiments. The advantage of magnetite is that can be collected through magnetic methods. In this way, wastes from different pyrometallurgical processes characterized by their high iron content could be treated through concentrated solar energy, and in this way, recovering iron from them as magnetite.

3. Solar energy in materials processing

This section will be dedicated to materials processing, especially metallic materials. First experiments in this line were based on melting materials (for instance, melting aluminum, tin and zinc, Gopalakrishna and Seshan, 1984, Suresh and Rohatgi (1979), 1981), or reaching the melting point of a certain metal or phase as we can read in the introduction section. Other studies in the field of materials processing are the surface modification by adding coatings. In this way, Armas et al.

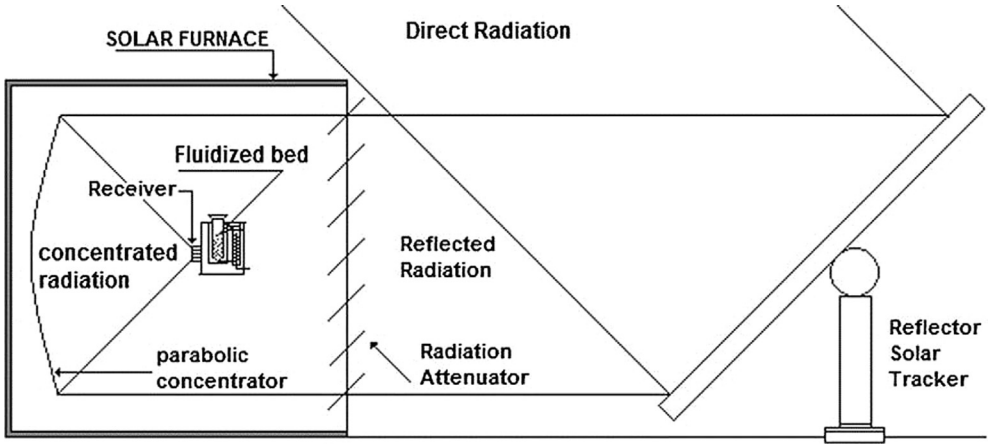

Fig. 4. Scheme of the solar installations used in the experiments (reprinted from Ruiz-Bustinza et al. (2013). Copyright 2013 John Wiley and Sons, Inc.).

(1976) studied the chemical vapor deposition of NbB_2 and TaB_2 by using concentrated solar energy as heating system. Recent studies regarding materials processing are described in this section.

3.1. Aluminum and titanium foams

Aluminum foams are a metallic material relatively isotropic and very porous with a random distribution of pores in their structure. Pores, essentially spherical and closed, occupy 50–90% of the total volume. Mechanical and physical properties depend on the density (typically in the range 0.4–0.8 g/cm^3). Aluminum foams are extremely efficient in sound absorption, electromagnetic protection, impact energy and vibration absorption, and they are not flammable and remain stable even at high temperatures (Gutiérrez-Vázquez and Oñoro, 2008). Aluminum foams can be divided into two types: closed pores, used in structural applications; open pores, used because of their specific properties (thermal, superficial, etc.). A high stiffness and soundproofing characterize aluminum foams of closed pores and can be manufactured by direct injection of gases in the molten metal or by means of using a foaming agent or a foamable precursor with the material in the interval solid-liquid (Gutiérrez-Vázquez and Oñoro, 2008). Obtaining aluminum foams from precursors, which were made through either melting or powder metallurgy via, requires their heating up to temperatures higher than the aluminum melting point. The objective is reaching the decomposition of the foaming agent dispersed in the matrix of the precursor and generating gas that causes the foaming of the molten aluminum. The interest of aluminum foams comes from their physical and mechanical properties, particularly high stiffness with low specific weight, high permeability to gasses combined with high mechanical strength. Besides, aluminum foams are also a relevant type of foams because of their low density, corrosion strength and low melting point (easily handle) (Gutiérrez-Vázquez and Oñoro, 2008).

García-Cambronero et al. (2008) and García-Cambronero et al. (2010) suggested the use of concentrated solar energy in the foaming of aluminum-silicon alloy. They used as initial raw material $AlSi_{10}$ with 0.8% of foaming agent (TiH_2). The mold (see Fig. 5), where the initial material is located, is loaded into the fluidized bed furnace (preheated with air up to 650–750 °C 2 h before the treatment), and initial material is foamed in 2–5 min (considering the following steps: put the mold into the furnace, holding time and fast removal from the furnace). The mold is water cooled down to the room temperature. The advantages of the process proposed by García-Cambronero et al. (2008) and (2010) are: foaming treatment faster than in preheated electric furnace; and foaming process at lower temperatures (670–700 °C) than in preheated electric furnace (750 °C). The fast heat transmission from the air to the mold justifies the advantages of the solar foaming process. In this line, García-Cambronero et al. (2004) foamed Al_7Si with marble or synthetic calcium carbonate ($CaCO_3$) as foaming agent. The welding of aluminum foams was studied by García-Cambronero et al. (2014). Aluminum foams were, as presented, widely studied by García-Cambronero et al. from the foaming process to the welding process with interesting results as the foaming process takes place at lower temperatures than in electric furnaces. The problem of the foaming process based on concentrated solar energy may be the size of the foam parts that could be obtained because it seems complicated obtaining sheets of aluminum foam (as those used in sound absorption). For that reason, the applications of aluminum foams obtained through concentrated solar energy seem limited to not big parts.

Foams were also studied by García et al. (2016a), but for titanium. They sintered porous titanium foams in a 2 kW parabolic concentrator under argon atmosphere. As raw materials Ti powder (99.9% purity, < 53 μm), NaCl crystals (600–1000 μm) and 2 wt.% PVA (Polyvinyl acetate) aqueous solution, as organic binder, were used. They were mixed in different weight proportions and cold compacted at 300 MPa for 2 min to obtain green pellets (20 mm in diameter and 15 mm in height). After that, green pellets were dried at 100 °C for 2 h, heated up to 400 °C for 2 h with the purpose of removing PVA, immersed in hot water at 80 °C for 18 h to dissolve the space holder and dried at 100 °C for 2 h. Sintering (see Fig. 6) was then performed at 750–800 °C in approximately 50 min, in shorter times and lower temperatures than in conventional furnaces. The obtained porosities were: 58–77%, with dual size (500–1000 μm and 1–10 μm).

3.2. Sintering

3.2.1. Copper sintering

Cañadas et al. (2005) studied the feasibility of using concentrated solar energy in copper sintering (see Fig. 7). As starting material, they used annealed electrolytic copper of low oxygen, disposed as coiled wire or straightened wire, under atmosphere slightly reducing. Cañadas et al. (2005) observed that coiled wire cannot be used because there was dilatation in the outside layers that caused discontinuities in the process. Straightened wire samples showed results like that obtained in conventional furnaces (Alexander and Balluffi, 1957). Continuing with the copper solar sintering process, Lacasa et al. (2006) designed the automatic control system for the process by using fuzzy logic models.

Although the research proposed by Cañadas et al. (2005) addresses their objective, and offers basic knowledge about how to proceed with copper and concentrated solar energy, there is a lack of continuity in the research. Concentrated solar energy could be competitive with modern high-energy technologies in nanostructured copper wires, for instance, Arnaud et al. (2016) proposed the obtaining of nanostructured

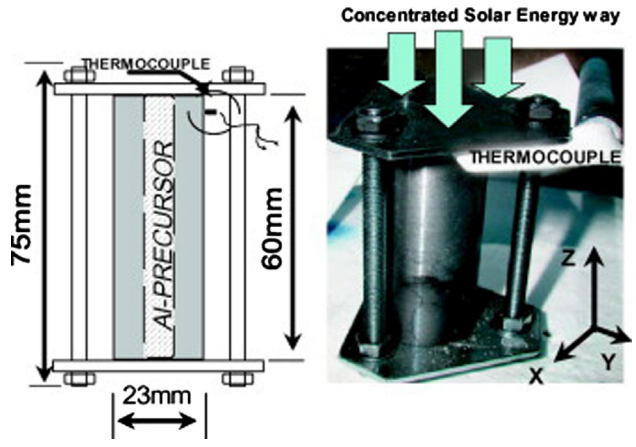

Fig. 5. Drawing and mold used in the foaming process (reprinted from García-Cambronero et al. (2010) with permission of Elsevier).

Fig. 6. Titanium foamed by using concentrated solar energy (reprinted from García et al. (2016a) with permission of Elsevier (Copyright 2016)).

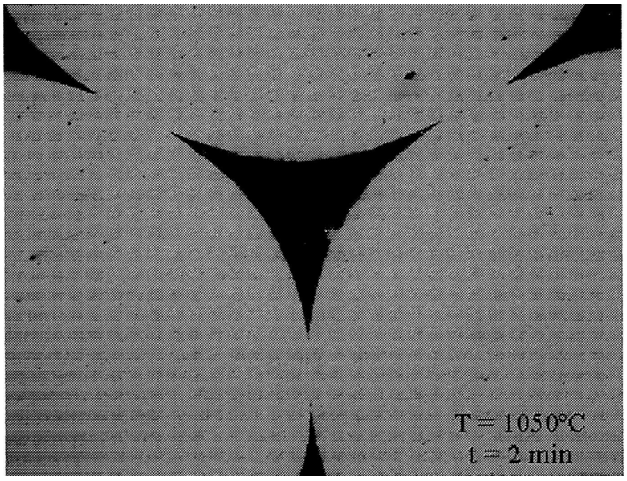

Fig. 7. Cross-section of wires after sintering for 2 min at 1050 °C in a solar furnace (from Cañadas et al. (2005) in Revista de Metalurgia).

copper wires prepared by spark plasma sintering.

3.2.2. Ni-Zn ferrites

Ni-Zn ferrites are soft magnetic materials used in electronic devices and magnetic equipment that are industrially manufactured by uniaxial pressure. Gutiérrez-López et al. (2010) studied the sintering of this material by means of concentrated solar energy. The starting material was a granulated pre-sintered Ni-Zn ferrite powder (mixture of Fe_2O_3, NiO and ZnO). Using this mixture, they manufactured green specimens with toroid shape (10.3 mm outer diameter, 5 mm inner diameter and 3.45 mm depth). Gutiérrez-López et al. (2010) carried out the experiments in the Plataforma Solar de Almería (Spain) controlling three variables: temperature (1150–1300 °C), heating rate (15, 30 and 60 °C/min) and time (15, 30 and 60 min). Gutiérrez-López et al. (2010) achieved a complete reaction in all experiments that they performed. They achieved, if compared with the process in electric furnace (2 h), a reduction in the sintering time of 90%, a denser product and better magnetic properties.

3.2.3. High speed steels

High speed steels are a kind of steel that can be used in tools for machining with swarf removing at great speed (higher than 30 m/min) (Pero-Sanz, 2004). This process produces heating in the tool during operation, and for that reason the tool must be extra-hard (63–68 HRC) and keep that hardness at high temperatures (around 600 °C) (Pero-Sanz, 2004). High speed steels are high alloyed steels whose manufacture is complex because of the complex chemical composition. High energy techniques can be applied for the manufacture of prototypes and short series tooling, reducing both time and costs. One of the high energy techniques is concentrated solar energy, which was used to manufacture high speed steels from powders and by means of a sintering process, and as described below results show reductions in processing times, reduction in processing temperatures and improvements in quality of the product.

Herranz et al. (2013) used metallic powders of high speed steel AISI M2 with size lower than 150 μm. Samples were compacted at 650 MPa with the purpose of obtaining green bars (31.6 mm × 12.8 mm × 2.4 mm) that were treated in the Plataforma Solar de Almería (solar furnace) and in the School of Industrial Engineering of the University of Castilla La Mancha (Fresnel lens). Samples were treated under controlled atmosphere (N_2-5%H_2) at temperatures between 1115 °C and 1200 °C with heating rates of 50 °C/min and holding times at maximum temperature of 30 min. Herranz et al. (2013) obtained densified parts at lower temperatures (1150 °C) than with the conventional procedure (around 1290 °C) in shorter times (90 min solar furnace, 30 min Fresnel lens, and 10 h conventional furnace). Herranz et al. (2013) also achieved higher hardness values (800–900 HV) if compared with conventional microstructures (620 HV). The reason is that fast heating and cooling rates caused the appearance of phases of submicron size (vanadium nitrides) that increased the hardness of the steel. Fast heating and cooling rates are one of the main advantages (or disadvantages depending on the material, for instance thermal shock risks can appear in certain materials) as the duration of the treatment can be shortened, but also because it is possible to obtain phases that could not be obtained through conventional methods (in this case, submicron phases). Fast heating and cooling rates, apart from allow metastable phases at room temperature also restrain the grain growth during the cooling period.

High speed steels compete with cemented carbides in several applications that include cutting tools for machining. Herranz et al. (2014) proposed the reinforcement of AISI M2 high speed steels with vanadium carbide by means of using concentrated solar energy. In this way, the addition of ceramic reinforces to a metallic matrix (AISI M2) gives as result a metal matrix composite with properties like those of the steels and cemented carbides. Herranz et al. (2014) sintered the same AISI M2 steel powders that were used in Herranz et al. (2013), and vanadium carbide powders (< 10 μm), which were mixed in proportions of 3, 6 and 10% wt. of vanadium carbide. Mixtures were cold pressed at 650 MPa obtaining a green compact of 4 mm thickness and 16 mm of diameter. Tests were performed as in Herranz et al. (2013) under N_2-5%H_2. Herranz et al. (2014) used a Fresnel lens, and treatment cycles of 30 min with fast heating rate (275 °C/min) up to the maximum temperature (870–1160 °C), holding time at maximum temperature of 15 min and fast cooling rate down to the room temperature. Herranz et al. (2014) carried out other treatment in solar furnace (Odeillo Solar Furnace) with duration of 15 min, with fast heating rate (735 °C/min) up to the maximum temperature (920–1050 °C), holding time of 5 min, and finally fast cooling rate down to the room temperature. Herranz et al. (2014) achieved by using concentrated solar energy a reduction in the sintering temperature without adding other elements such as graphite (1140–1295 °C required in conventional furnaces; between 940 °C and 1150 °C in the case of Fresnel lenses, depending on the vanadium carbide addition (maximum temperature when 0% VC and minimum temperature when 10% VC); 990 °C when solar furnace and 3% VC and 975 °C when 6% VC). Herranz et al. (2014) observed an increase in the hardness of the obtained product (between 620 ± 30 $HV_{0.2}$ and 880 ± 30 $HV_{0.2}$, conventional furnace; between 940 ± 30 $HV_{0.2}$ and 990 ± 30 $HV_{0.2}$, Fresnel lens depending on VC addition; between 910 ± 30 $HV_{0.2}$ and 930 ± 30 $HV_{0.2}$, solar furnace with 3% VC and 6% VC respectively). This improvement in the hardness is consequence of the affinity between vanadium and nitrogen (carbon is liberated during the process, and new carbides, carbonitrides and nitrides are formed by reaction with alloying elements in the steel during the process), and the formation of submicron and nanometric particles during the process. Herranz et al. (2014) also observed a reduction in the duration of the treatment (10 h in conventional treatment, 30 min with Fresnel lenses and 15 min in solar furnace).

The reduction in processing times was also observed by García et al. (2016b). They prepared mixtures of AISI M2 high speed steel and vanadium carbide (3, 6 or 10 wt%) through powder metallurgy and concentrated solar energy, and compared results with the same samples obtained in a tubular electric furnace. As mentioned, processing times were reduced, but also samples with better wear properties were obtained (due to the refinement of the microstructure and appearance of carbonitrides).

3.2.4. Titanium

This section will be dedicated to the sintering of titanium and titanium compounds by using concentrated solar energy. As observed in other materials, reductions in time and temperature for the sintering process, if compared with conventional methods, are observed. Apostol

et al. (2015) developed a process to grow $MgTiO_3$ nanostructured thick films (that could replace bulk ceramic components in electronic applications) that combines solar physical vapor deposition (SPVD, read in Westwood (1989) about Physical Vapor Deposition) and electrophoretic deposition (EPD, read in Besra and Liu (2007) about Electrophoretic Deposition). SPVD was used to synthesize nanopowders, while EPD was used to prepare thick films (18–20 μm). They observed promising dielectric properties, and decreases in sintering temperature in comparison to conventional solid-state reaction temperature. In the same line, Apostol et al. (2018) sintered magnesium titanate ceramics in solar furnace. They sintered $(MgO)_{0.63}(TiO_2)_{0.37}$, $(MgO)_{0.49}(TiO_2)_{0.51}$ and $(MgO)_{0.50}(TiO_2)_{0.50}$ ceramic samples in air at about 1100 °C for 16 min, 1 h, 2 h and 3 h. They obtained $MgTiO_3$ geikielite by solar sintering of $(MgO)_{0.63}(TiO_2)_{0.37}$ at 1100 °C (16 min-30 h). This sample sintered at 1100 °C for 3 h exhibited well-sintered, non-porous and good density. And, in the case of sintering only titanium powders, Kovacik et al. (2017) tested the solar sintering of titanium (Hydrogenation-Dehydrogenation Ti powder, HDH Ti powder) by using concentrated solar energy. They observed porosities below 5%, and sintering times were shorter than in vacuum furnace. Radial shrinkage was almost the same than in the vacuum furnace samples, but axial shrinkage was 20% higher due to that argon gas used during the sintering at high temperature remains enclosed in the pores.

3.3. Coatings

A coating could be defined as a cover that is applied to the surface of an object, in this case a metal (substrate), with the purpose of improving the functional properties of that base metal, for instance wear resistance or corrosion resistance. In this section, the coating processes based on concentrated solar energy will be described.

3.3.1. Molybdenum

Pantelis et al. (2005) proposed the surface alloying of a stainless steel 304L by using molybdenum powders and concentrated solar energy. Molybdenum is used as alloying element in steels as improves hardenability and toughness , but also improves the corrosion and wear resistances. Pantelis et al. (2005) used as starting materials stainless steel 304L (layer) and molybdenum powders (90 ± 15 μm; 75% Mo, 25% Ni, Cr, B, Si and Fe (wt.)) in a 1 mm thickness layer and carried out experiments in the Plataforma Solar de Almería. Argon atmosphere was used in all tests, 1300 °C was the maximum temperature, heating rate varied between 7.2 and 3.6 °C/s and holding time was varied between 0 and 6 min. Pantelis et al. (2005) observed a good adherence to the 304L stainless steel layer with bubbles but without visible cracks in all cases. When fast heating rate (7.2 °C/s), Pantelis et al. (2005) observed that the treated zone reached 800 μm in depth with low porosity, without cracks but with un-melted molybdenum areas and heterogeneity in the hardness values (400–700 HV_{300}). When slow heating rate (3.6 °C/s), Pantelis et al. (2005) observed that the un-melted molybdenum areas disappeared and there was homogeneity in the hardness values (370 HV_{300}). Pantelis et al. (2005) checked that when the holding time at 1300 °C was 3 min the treated area reached 1100 μm in depth with two zones clearly different: the upper one of 400 μm in depth was characterized by being fine grained with high hardness (600–780 HV_{300}); and the lower one of 700 μm in depth was characterized by being coarse grained and having lower hardness (500 HV_{300}). Finally, Pantelis et al. (2005) observed that when the holding time was 6 min the depth of the treated zone reached 1400 μm without differenced zones, being a homogeneous coating of 300 HV_{300}. The problem of using concentrated solar energy in preparing coatings is the surface that could be coated. Considering the 1.5 kW Odeillo solar furnace, the area of the beam of concentrated solar energy has approximately 15 mm in diameter, so or parts are small or achieving a coating in large surfaces would take a long time. Pantelis et al. (2005) achieved satisfactory results regarding the quality of the coating but nothing is mentioned about the industrial possibilities of this technique (only that good results were obtained if compared with other surface treatment processes as laser irradiation), but probably would be limited to short series tools.

3.3.2. Cast irons

Nodular cast irons are competitive with steels in some applications due to the low cost and good mechanical properties, especially the austempered ductile irons (ADI) (Pero-Sanz et al., 2018). Yu and Lu (1987) studied the coating of nodular cast iron by using tungsten carbide powders melted by the action of concentrated solar energy. The hardness values reached 1000 $HV_{0.2}$ and wear resistance was improved. The coating of nodular cast irons by using concentrated solar energy could be useful in certain applications, although as mentioned in other sections the problem of using this energy source in coating is the surface that could be coated (coatings might be limited to small parts and short series of product). Moreover, by conventional methods, it is possible to obtain nodular cast irons with excellent wear properties (Pero-Sanz et al., 2018). Cast irons when alloyed with chromium allow reaching hardness values close to that mentioned by Yu and Lu (1987), being these alloys used when wear and abrasion resistances are pursued.

3.3.3. Nitriding

Titanium and its alloys are interesting as structural materials because of their excellent chemical and mechanical properties, having low density (4.51 g/cm^3) and high melting point (1675 °C). However, because of both the low friction coefficient and low wear resistance they have limited applications. Several methods have been developed with the purpose of improving its hardness and wear resistance, being the thermochemical treatment the most common. Rodríguez et al. (2013) proposed the use of solar energy in gaseous nitriding (thermochemical conversion treatment that requires heating the titanium alloy up to high temperatures for long periods under controlled atmospheres) as an alternative to conventional techniques or advanced techniques that use plasm, lasers, or microwaves. The solar nitriding of titanium alloys was also previously studied by Sanchez-Olías et al. (1999), García et al. (1998) and (1999) (they obtained uniform 6 μm films of TiN and $TiN_{0.3}$ in treatments that lasted 2 min by using a Fresnel lens solar installation; the growing rate is faster than in conventional treatments and similar to that obtained in induction furnaces and high power lasers).

Rodríguez et al. (2013) used Ti_6Al_4V alloy discs (5 mm in thickness and 16 mm in diameter) as starting material in as received (rolled and annealed) condition with biphasic grain structure (α + β) and 400 HV hardness. The treatment was performed in a Fresnel lens solar installation, which allowed 264 W/cm^2, and using a chamber with controlled atmosphere (N_2-5%H_2). Rodríguez et al. (2013) carried experiments at: 1100, 1150 and 1200 °C with holding time of 10 min; and, at 900 and 1200 °C with holding time of 15 min. The effect of the time was studied in samples heated up to 1200 °C and held at that temperature for 5, 10 and 15 min. Rodríguez et al. (2013) identified three regions: external layer of δ-TiN, intermediate layer of α-Ti(N) and metal base (see Fig. 8). The highest hardness (2100HV) was reached when samples were heated up to 1200 °C for 15 min, while achieving that hardness value in electric furnace would take 8 h. The improvements in time observed for this process, accompanied with the reduction in energy costs, make of the titanium nitriding a promising solar process.

3.3.4. Self-propagating high-temperature synthesis (SHS)

NiAl has excellent mechanical properties accompanied by a high melting point, excellent corrosion resistance and good oxidation resistance at high temperatures. For all that reasons, NiAl has applications in aeronautics or energy conversion. Typical method of obtaining NiAl is by means of self-propagating high-temperature synthesis that consists in a series of highly exothermic reactions of the initial reagents that transform spontaneously into the products once initialized. In this way, Rodríguez et al. (1999) proposed the use of solar energy as initializing energy.

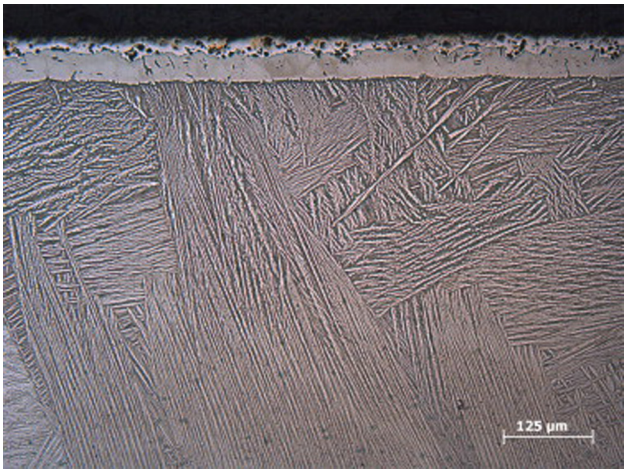

Fig. 8. Solar nitrided sample (reprinted from Rodríguez et al. (2013) with permission of Elsevier (Copyright 2013)).

Rodríguez et al. (1999) used a Fresnel lens allowing power densities of 220–260 W/cm^2. Specimens were made of carbon steel (16 mm in diameter and 5 mm in height) with the powders of 50% Ni (< 10 µm)-50% Al (-75 + 45 µm) (% at.) placed in a slot of 2 mm in depth and 14 mm in diameter that were pressed at 200 MPa (10% wt. of NiCrAl was added with the purpose of reducing the porosity). Rodríguez et al. (1999) obtained homogeneous coatings with microporosity due to the remaining gases in the final solidification zones (a reduction of the porosity was not observed with the addition of 10% NiCrAl) and a depth of the coating of 750 µm.

Sierra and Vázquez (2005) used a Fresnel lens as Rodríguez et al. (1999) with the purpose of studying the influence of the Ni-Al mass. Specimens were drilled cylinders of steel (16 mm in diameter and 5 mm in height with a hole of 14 mm in diameter and 3 mm in height). They used mixtures of Ni (< 10 µm) and Al (< 30 µm) in molar ratio 1:1, loaded in the hole and uniaxially pressed at 300 MPa. Sierra and Vázquez (2005) studied three masses: 0.3 g, 0.6 g and 1.7 g, and observed that: when the mass was 0.3 g, there was not adherence; when 0.6 g., there was adherence but not in the interphase; while when the mass was 1.7 g, a good adherence seemed to exist as it was not possible to see cracks. Sierra and Vázquez, 2005 observed that when the mass was 0.3 or 0.6 g the coating had small pores. However, when the mass used was 1.7 g, there were few pores but with some of them lengthened. The lack of adherence observed when using little masses of NiAl is due to the low heating of the steel (low energy released by the SHS process), and for that reason, the absence of diffusion towards the substrate.

Sierra and Vázquez (2005) observed problems of adherence in some cases, so Sierra and Vázquez (2006) studied the improvement in the adherence of the NiAl coating by placing a layer of Ni between the base metal and the coating. Sierra and Vázquez (2006) used as in the other cases a Fresnel lens and low carbon steel specimens with a hole, where they loaded, first 0.3 g of Ni and pressed uniaxially, and then loaded the mixture Ni-Al (1:1 M ratio) and pressed uniaxially at 300 MPa. Tests were carried out under inert (N_2) or vacuum (70 mbar) atmosphere. Sierra and Vázquez (2006) observed a good adherence in all coatings because of that the energy released by the SHS process melted the Ni layer, and heated the steel favoring the diffusion Fe-Ni and promoting the good adherence. An intermediate layer of Ni_3Al between the Ni layer and the coating of NiAl was observed in this coating. The coating had low intrinsic porosity (formed due to the lower volume of the final products in the interface Ni/NiAl) and low extrinsic porosity (formed due to the air trapped in the products). Considering the atmosphere effect, Sierra and Vázquez (2006) observed that under vacuum atmosphere there were several superficial elevations that deformed the coating. On the contrary, superficial irregularities due to internal bubbles were observed when N_2 atmosphere was used and the weight of the Ni-Al mixture was higher than 2.2 g.

Sánchez-Bautista et al. (2006) studied the obtaining of large surfaces coated with good adherence and low porosity. They used a 2 kW Odeillo solar furnace that allowed 1600 W/cm^2 of power density in a spot of 15 mm in diameter, and rectangular specimens (55 mm × 6 mm × 2 mm) with a hole loaded with Al-Ni powders (1.5–2.0 g in molar ratio 1:1) and pressed at 300 MPa. Specimens moved below the concentrated solar energy focus at a controlled speed (1–2.5 mm/s), always under argon atmosphere. Sánchez-Bautista et al. (2006) observed that the higher the power density, the lower the porosity and the higher the adherence.

3.4. Joining technologies

As happens in other processes the main problem of solar energy is the discontinuity of the sun radiation (day-night, weather, season, etc.) that impedes the application of the concentrated solar energy in processes where huge amount of materials must be treated. In the particular case of joining technologies, concentrated solar energy could not be applied in the manufacture, for instance, of cars that are produced in factories operating 24 h 365 days yearly, but could be applied to high added value or to small series of products, as for instance in precious materials or other high added value products. Even when high-power technologies, as lasers, are being used in welding the limitations of concentrated solar energy can be mainly found in the sun availability and in the location of sun best conditions. Solar welding was achieved satisfactorily in the case of steel, aluminum and titanium alloys, but the possibility of scaling-up the results to industrial level was not studied, and this question should be considered if there is a real interest in using concentrated solar energy in welding. Moreover, fast heating and cooling rates should be considered as non-equilibrium phases could appear and this question might be a problem because sometimes these phases could make brittle the joint. Below, it is possible to read the description of different welding processes performed by means of concentrated solar energy by varying: the geometry of the joints or the materials to be welded.

Kaddou and Abdul-Latif (1969), studied the feasibility of joining metals by using solar energy. They carried out the experiments in a Fresnel lens solar installation that allowed temperatures of around 1095 °C. Kaddou and Abdul-Latif (1969) planned to join metals by soldering, brazing and welding (accomplished by the increasing temperature of the process), and using lead tin solder. They tried several kinds of joint such as butt, lap and edge, as well as two twisted wires and rod joined to a flange. Kaddou and Abdul-Latif (1969) found that thin metal strips (< 3 mm) of mild steel, brass or copper were easily soldered. One of the main features of the solar furnace is the feasibility of using the desired atmosphere (vacuum, inert, reducing or neutral). However, one of the main drawbacks is the high reflectance of bright metals that require the blackening of the surface. **Kaddou and Abdul-Latif (1969)** also tried silver soldering but without positive results because of the high melting point of the solder, which was impossible to be reached due to the limitations of the solar furnace that they used. Kaddou and Abdul-Latif (1969) observed during soldering of cold rolled strips that were locally softened due to recrystallization and annealing processes. This adds a possible application of solar furnaces for stress relieving or annealing process in cold worked metals.

Kim et al. (2004) carried out experiments where they joined engineering thermoplastic materials by applying concentrated solar energy. This line could be interesting as temperatures required in plastics/polymers industry are usually lower and maybe required powers could be lower. This way, the application of concentrated solar energy could be spread to regions with lower values of irradiation.

Karalis et al. (2005) proposed the use of concentrated solar energy in joining 7075 aluminum alloy (7075 aluminum alloy is widely used in building thin structures of welded aluminum with outstanding

mechanical behavior). They used 7075-T6 aluminum blocks of 56 mm × 36 mm × 26 mm and 7075-T6 aluminum plates of 56 mm × 36 mm × 2 mm. Karalis et al. (2005) used a 2 kW solar furnace and a table that moved below the focal point (20 mm). Experiments were carried out under argon atmosphere and glass chamber. Karalis et al. (2005) did two experiments: weld bead in the block (0.3–1.2 mm/s displacement speed of the sample below the focus) and welding block-plate (0.45 mm/s). Karalis et al. (2005) observed a partial welding with low penetration and strength. Changes in the microstructure and softening were also observed. Karalis et al. (2017) attempted the welding of aluminum 5083-H111 alloy plates by using variable concentrated solar energy, controlling the heat input and preventing the entire melting of the plates. They observed that metallurgical bonding was not achieved because of the formation of a refractory film of alumina along the weld centerline. Pantelis et al. (2017) used concentrated solar energy to weld thin plates of 6082 aluminum alloy. They designed both a vacuum chamber and a cooling system to achieve an inert atmosphere and suitable heat dissipation. Microhardness and ultimate tensile strength were reduced a 23% and 32% respectively in the butt compared with the base metal, but this reduction is in good correlation with other fusion weld methods.

Romero et al. (2013) welded high temperature melting point materials such as AISI H13 tool steel and AISI 316L stainless steel. They used specimens of 60 mm × 60 mm × 3 mm and 30 mm × 60 mm × 5 mm in the case of using AISI H13 steel, while used specimens of 30 mm × 60 mm × 1.5 mm for AISI 316L. As filler material, they used low carbon steel filler CITOFIX E6013 rod (4.8 mm diameter). **Romero et al. (2013)** attempted three welded joint designs (flush corner joint, T- joint, and V-grove butt joint) in AISI H13 steel, while in AISI 316L only welding on flush corner joint was attempted. Romero et al. (2013) used a 2 kW vertical axis concentrator (15 mm diameter of focal point) with radiations among 500 and 990 W/cm^2, with specimens placed in a quartz chamber under argon atmosphere to avoid surface oxidation. Specimens displaced below the spot of concentrated solar energy at speeds between 0.3 and 1.2 mm/s. Romero et al. (2013), as opposed to Karalis et al. (2005) for aluminum alloy welding, achieved full penetration of welded beads on AISI H13 steel and AISI 316 stainless steel without any defects for the different joint configurations.

Romero et al. (2015) welded sheets (30 mm × 60 mm × 5 mm) of Ti_6Al_4V titanium alloy in flush corner joint configuration by means of using a 2 kW solar furnace. As in previous experiments, inert argon atmosphere was used. Romero et al. (2015) achieved a full penetration of welded tracks without defects when they used a tracking speed (displacement speed below the solar spot) of 0.15 mm/s and a solar radiation of 1000 W/cm^2.

3.5. Cladding

Cladding is a welding procedure based on putting weld metal on the surface of the part, making a coating of the base metal. The objective of the cladding is increasing either corrosion or wear resistances. Fernández et al. (1998) studied the cladding of AISI 4140 steel with powders of Ni superalloy, in a 60-kW solar furnace in the Plataforma Solar de Almería. They tested cylindrical samples of 35 mm in diameter and different heights (15, 25 y 35 mm) with a hole of 2 mm in depth and 29 mm in diameter, where Ni superalloy powders were placed and pressed. Tests were conducted under non-oxidizing atmosphere, and for different times (300–480 s) and solar power densities (691–827 kW/m^2). They observed that powder melt and cladding was obtained.

Ferriere et al. (2006) proposed the utilization of concentrated solar energy in cladding processes as an alternative to lasers because of its efficiency (70% solar furnace, 2% lasers) and installation costs for powers between 1 and 50 kW_{th} (1.5 €/kW_{th} solar furnace, 100 €/kW_{th} laser sources). Ferriere et al. (2006) carried out experiments in a 2 kW solar furnace at Odeillo using as base metal carbon steel (Fe-1.2%C) and powders of AISI 316 austenitic steel (17Cr12Ni2.5Mo1Si0.1C). Specimens were blocks of 60 mm × 10 mm × 8 mm with a slot of 55 mm × 6 mm × 2 mm, where the powders were deposited and cold pressed (200 MPa). Ferriere et al. (2006) treated the samples under vacuum conditions with the purpose of preventing oxidation, and displacement speeds under the concentrated solar energy focus of 0.8–2 mm/s. Ferriere et al. (2006) observed that when displacement speed was 0.8 mm/s there were problems of losing material by vaporization (Cr < 10%, Ni < 7%), and the structure had low corrosion resistance because Cr < 12%. The best results were found when displacement speed was 1.8 mm/s (faster speeds caused problems of adherence), there were not problems of losing material by vaporization as Cr = 13.4%, Ni = 10.3%, Mo = 2% and Si = 1.85%, and corrosion resistance was excellent.

3.6. Surface treatment in steels

Solar energy has been studied in thermal treatments for more than 30 years. Surface quenching is a widely used treatment to improve wear resistance of steel parts. This treatment may be carried out using conventional heating methods (flame and electromagnetic induction) and high-density energy beams (laser, electron beams, plasmas, etc.). In all cases, the source of heat should be sufficiently powerful to ensure that only the superficial layer of the part heats up to a higher temperature than the austenizing temperature. After cooling down, only the zones of the part that were austenized will have undergone the martensitic transformation that results in the hardening. In the internal zones, microstructural transformations would not have taken place, so mechanical properties would remain unchanged. In the Table 3, it is possible to find contributions in surface treatment of steels.

4. Solar energy in ceramics

As it is possible to see in the introduction section, reaching the melting point of high melting point ceramics was one of the first uses of concentrated solar energy. This section will be devoted to more recent concentrated solar energy applications in the field of ceramics.

4.1. Cordierite

Cordierite ($2MgO2Al_2O_35SiO_2$) was discovered in 1813 by Louis Cordier. This material is characterized by its low thermal expansion coefficient ($7 \cdot 10^{-7} K^{-1}$) in the range of temperatures between 298 K and 1273 K, and by its excellent thermal-shock resistance ($\Delta T > 350$) (Ashton Acton, 2013; Costa-Oliveira et al., 2009). The main applications of cordierite are multilayer circuit boards, catalytic converters, diesel particulate filters, kiln furniture, thermal insulation parts, etc. (Ashton Acton, 2013; Costa-Oliveira et al., 2009).

Costa-Oliveira et al. (2005) sintered at 950 °C commercial powders for the formation of cordierite through concentrated solar energy, but they observed that cordierite was not formed and checked that heating rate had critical importance in the process, the same as the starting materials and the processing temperature. Costa-Oliveira et al. (2009) sintered a commercial material, which included ball clays, talc, feldspar, alumina, and silica, by heating at temperatures up to 1573 K. These powders were cold pressed at 45 MPa with the purpose of preparing discs (30 mm diameter and 2.5 mm thickness). To avoid cracking and non-homogenous sintering, Costa-Oliveira et al. (2009) covered the discs with a part of zirconia, avoiding direct exposition to solar radiation. The main advantage of the process proposed by Costa-Oliveira et al. (2009) is the reduction in the duration of the treatment from 24 h using conventional methods to 60 min using solar energy. Costa-Oliveira et al. (2009) also observed that properties of solar sintered cordierite discs if compared with conventional cordierite discs were similar. As happens in other sintering processes, the method proposed by Costa-Oliveira et al. (2009) could find application in short series of parts.

Table 3
Surface hardening in steels by using concentrated solar energy,

Reference	Country	Solar Installation	Power density (W/cm^2)	Type of steel	Duration	Dimensions	Hardened zone
Yu et al. (1982)	China	Parabolic disc	3000	High carbon or low alloy (T8A, T10A, 40Cr, 20Cr, QT60-2, 30CrNi3)	1–7 s (several passages, risks of overlapping)	30–40 mm in diameter, and 1.35–5 mm in thickness	5 mm diameter, 0.5 mm in depth
Maiboroda et al. (1986)	Ukraine	1.5 kW Parabolic disc	200–400	34KjN3MFA (parts of machinery). Samples were annealed at 860–880 °C for 2 h, cooled inside the furnace and tempered at 640 °C for 2 h, and then cooled in water. After this treatment, samples had 37–39 HRC of hardness.	–	–	950–1000 °C were reached on the surface, and then, samples were air cooled in 3–5 min. Hardness rose to 53–55 HRC, and ductility improved in areas near to the surface
Pitts et al. (1988) and Stanley et al. (1989)	USA	Solar furnace	200	AISI 4130 and A2 steel for tools	6 s	Cylindrical (50 mm in diameter and 1.6 mm in thickness) and rectangular (610 mm × 150 mm × 13 mm)	1–2 mm in depth
Rodríguez et al. (1995)	Spain (PSA)	Tower and heliostats field	80	AISI 4140 steel	Different (83–200 s)	35 mm in diameter and 35 mm in height	Similar results than conventional techniques of surface hardening. Fully martensitic transformation after water cooling was achieved, while in large samples self-quenching is also possible. (< 15 mm in depth)
Yang et al. (1996)	Spain (PSA)	Solar furnace	–	EN24, EN8, EN16 (tested, not hardened)	–	Cylinders (12.5 mm in thickness and 25 mm in diameter)	–
Rodríguez et al. (1997)	Spain (PSA)	Solar furnace	180–250	Low alloyed, 40CrMo4 (samples were normalized and tempered with the purpose of homogenizing the structure before the solar treatment. Samples were painted (black painting, Pyromark 2500) for improving the absorption of energy.)	20–45 s	Cylindrical samples (35 mm in diameter; 35 mm in height)	The hardness after the treatment reached 60 HRC, which was like that one achieved in a conventional furnace. Microstructurally (depth from the surface): 0.5 mm, only martensite is found (fine grain, full transformation); 1.75 mm, ferrite in the structure of martensite is observed (partial austenization); 2 mm; the original bainite with small amount of martensite is found; and 2.5 mm, the microstructure was the original one.
Ferriere et al. (1999)	France	Solar furnace	1300	Carbon steel	2–4 s	Rectangular samples (20 mm × 20 mm × 60 mm)	0.4–1.15 mm in depth
Llorente and Vázquez, 2009	Spain (Madrid)	Double reflection Fresnel lens, with 1000x concentration factor	100 (max.)	AISI 1055 and AISI 4135 steels	See column Hardened zone	Cylindrical samples of 10 and 20 mm in diameter and 50, 60, 70, 75 and 100 mm in height	Dynamic, static, and localized tests were performed. Several types of samples were considered: type 1, 20 mm in diameter and 50 mm in length (AISI 4135 steel), 4–5 min exposure, static test, water-quenched (90 W/cm^2) showed an uniform hardened zone; type 2, 20 mm in diameter and 60 mm in length (AISI 1055 steel), dynamic test, successfully hardened and then tempered, hardness similar to that obtained through conventional methods; types 3 and 4, 20 mm in diameter and 75 mm in length, and 20 mm in diameter and 100 mm in length, respectively, are too big for the concentrator; types 5 and 6, 10 mm in diameter and 70 mm in length, and 10 mm in diameter and 100 mm in length, respectively (AISI 1055), locally hardened, extremes of the samples unaffected and some cracks on the surface.

4.2. Hard refractory ceramics

Metallic carbides and nitrides of high melting point are characterized by their high hardness, corrosion resistance, melting point and low thermal expansion coefficients. For that reason, they have interest in high temperature applications like turbines, engine parts or as protective coatings. The commonly used procedure for obtaining ceramic nitrides is by means of direct nitriding of the metallic element in presence of N_2 or NH_3 (Martínez et al., 1999 studied the synthesis of silicon carbide, tungsten carbide, titanium carbide and titanium carbonitride under controlled atmosphere of N_2 and Ar from metal powders and amorphous carbon; Shohoji et al. (2011) and Costa-Oliveira et al. (2012) studied the reactions of Ti, V, Nb and Ta with N_2 gas at 2000 °C and synthesized carbon-nitrides of these elements; Shohoji et al. (2013) synthesized nitrides of molybdenum and iron in ammonia (NH_3); Costa-Oliveira et al. (2015) experienced in nitriding of VI-group metals (Cr, Mo, and W) in ammonia). In a similar way, carbides are obtained by means of direct reaction among metal and carbon, or by vapor deposition techniques. However, both processes (nitride and carbide synthesis) require the previous synthesis of the metal from the oxide, generally by electrolysis. A different process from those previously described was proposed by Paizullakhanov and Faiziev, 2006 for the obtaining of calcium carbide from limestone and petroleum coke by using concentrated solar energy.

First research experiences in the synthesis of carbides and nitrides were those proposed by Murray et al. (1995). They studied the obtaining of a series of metals, carbides, and nitrides through solar energy by reaction of a series of metallic oxides (SiO_2, Al_2O_3, TiO_2, ZrO_2, MgO, ZnO and CaO) with carbon under N_2 and argon atmospheres. Experiments in argon atmosphere were carried out in a 7 kW solar furnace at the University of Minnesota (Fig. 9A), while experiments under N_2 atmosphere were performed in a 15 kW solar furnace at the Paul Scherrer Institute (Fig. 9B). Mixtures were prepared with excess of carbon over the stoichiometric, with fast heating rate up to the test temperature, where samples were maintained at maximum temperature for different times depending on the sample, and then were fast cooled down to room temperature under Ar or N_2 atmosphere. According to the initial mixture of oxides, it was possible to stablish the following results considering N_2 atmosphere: *SiO_2-C-N_2 system* (two experiments at 1773 K for 1.5–2 h), they obtained α-Si_3N_4 and SiC; *Al_2O_3-C-N_2 system* (two experiments: one at 1773 K for 1 h; and, the other with the following conditions, 0.5 h 1850 K + 0.5 h 1775 K + 0.5 h 1725 K), they observed similar results in both cases with a certain amount of Al_2O_3 with AlN in the products; *TiO_2-C-N_2 system* (three experiments, one at 1473 K for 1 h, other at 1773 K for 1 h, and the third at 1673 K for 2 h), they only observed TiN with neither TiC nor TiO_2; *ZrO_2-C-N_2 system* (one experiment at 1775 K for 0.5 h, other at 1750 K for 0.75 h, and the third one at 1775 K for 1 h + 0.75 h at 1850 K), they observed a mixture of ZrO and ZrN with certain amount of unreacted ZrO_2 in the first two experiments, while in the third one, they only found ZrN and ZrO. Under argon atmosphere, Murray et al. (1995) performed the following experiments: *Al_2O_3-C-Ar system* (2000 K and 0.2 atm), they observed Al_4O_4C, Al_2OC and Al_4C_3 without Al in the products (this element appeared only condensed outside of the crucible in small amount); *TiO_2-C-Ar system* (2240 K, 0.02 atm and 0.2 h), they observed TiC and Ti_2O_3 in the products without TiO_2; *SiO_2-C-Ar system* (2 min at 1850 K under 0.6 atm + 20 min at 2230 K under 0.03 atm), they obtained β-SiC and α-SiO_2; *ZnO-C-Ar system* (three experiments: one at 1550 K for 0.5 h, other at 2040 K for 5 min, and the third at 2080 K for 15 min under 0.1 atm), the presence of Zn (13%, 42% and 62% of the initial in the mixture, respectively), ZnO and C (graphite) were observed in the three experiments; *MgO-C-Ar system* (two experiments: one at 2234 K for 0.5 h under 0.04 atm, and the other at 2180 K for 30 min under 0.02 atm), they observed Mg (9% and 13% of the initial in the mixture, respectively), MgO and C (graphite) in both cases. As it was described in the first lines of this section, solar nitriding of metallic elements in presence of N_2 or NH_3 is the option for obtaining carbo-nitrides of certain metallic elements (Shohoji et al., 2011 and Costa-Oliveira et al., 2012, Ti, V, Nb and Ta; Shohoji et al., 2013, Mo and Fe; Costa-Oliveira et al., 2015, Cr, Mo, and W). Shohoji et al. (2012) also studied (following the line of this research group, prolific in this field) the carbo-nitride synthesis of some d-group transition elements (Ti, Zr, V, Nb, Mo and W) under N_2/Ar gas mixture, 1600 °C of processing temperature, and mixtures graphite/metal in the ratio 1.5/1. Carbo-nitride was detected for Ti, while for V and Nb, the presence of mono-carbide was the single phase detected. The formation of higher carbide, among several options of carbide phases, is that detected for Mo and W. Shohoji et al. (2013) studied the synthesis of Mo and Fe nitrides in flowing ammonia as in nitrogen gas environment it is not possible even at elevated partial pressure. δ-MoN range of formation is found between 700 °C and 800 °C, while in laboratory or industrial electric furnace the range of formation is a narrow window around 700 °C. ε-Fe_2N formation did not widen from around 500 °C compared with that in laboratory or industrial electric furnace. Costa-Oliveira et al. (2015) studied the nitriding of Cr, Mo and W under NH_3 gas flowing at 600–800 °C, as nitriding is not easily achieved in presence of nitrogen gas. The MoN was obtained in the range of temperatures described in Shohoji et al. (2013), the synthesis of WN was not possible in NH_3 at any examined temperature but W_2N was observed, and CrN/Cr_2N were observed for the Cr specimen. Costa-Oliveira et al. (2016) studied the nitriding of Ti and Zr in flow of NH_3 at low temperature (600–800 °C) and short time (30–90 min). They observed partial nitriding of Ti and Zr at 800–700 °C, but not at 600 °C. Fernandes et al. (2016) studied the solar nitriding of V, Nb and Ta in NH_3 gas flowing. They observed after 90 min of heating up to 800 °C a certain extent of the nitriding process for all specimens.

Particular carbides, characterized by their high hardness and refractoriness, are described below. These solar carbides and nitrides could have interest as they are produced in short series, and in competitive process conditions if compared with that required in conventional processes. The photochemical effects in some reactions under solar radiation as those described by Rodríguez et al. (2001) should be considered (formation of Ta_2C and TaC in the carburization of Ta with amorphous carbon; MoC formation at a temperature lower than that proposed in the equilibrium diagrams (**Guerra-Rosa et al., 1999**); acceleration of the amorphous carbon graphitization during the carburization of W (Shohoji et al., 1999; Shohoji et al., 2000)), as they could lead to new products or processes that cannot be obtained/performed in traditional industrial technologies.

4.2.1. Silicon-based materials

Silicon-based materials are part of a generation of ceramic materials with formulations that cannot be found in the nature and must be artificially sintered. The appearance of silicon carbides and nitrides is related with the topic *New Ceramic Materials* that can be found in the market since Edward G. Achenson founded in 1895 the Carborundum Co. (Verdeja et al., 2014). These materials are characterized by: synthetic raw materials, starting powders of high purity and small size, sintering temperatures between 1600 and 2200 °C, and uniform microstructure with minimum porosity (Verdeja et al., 2014). As mentioned, **Murray et al. (1995)** studied the silicon carbide and silicon nitride synthesis through concentrated solar energy, and they stablished the basic knowledge about carbides and nitrides under this source of energy. Here it is possible to see development of these researches of Murray et al. (1995) performed by other researchers.

4.2.1.1. Silicon Carbide (SiC). Silicon carbide is widely used in materials science and engineering, including composite materials, combustible cells, aircrafts, rockets, nuclear industry, electronics, and semiconductors industry. This large number of applications is consequence of its good absorbance, specific surface area, porosity, hardness, melting point, thermal conductivity, mechanical strength, and oxidation resistance, as well as its excellent chemical stability at

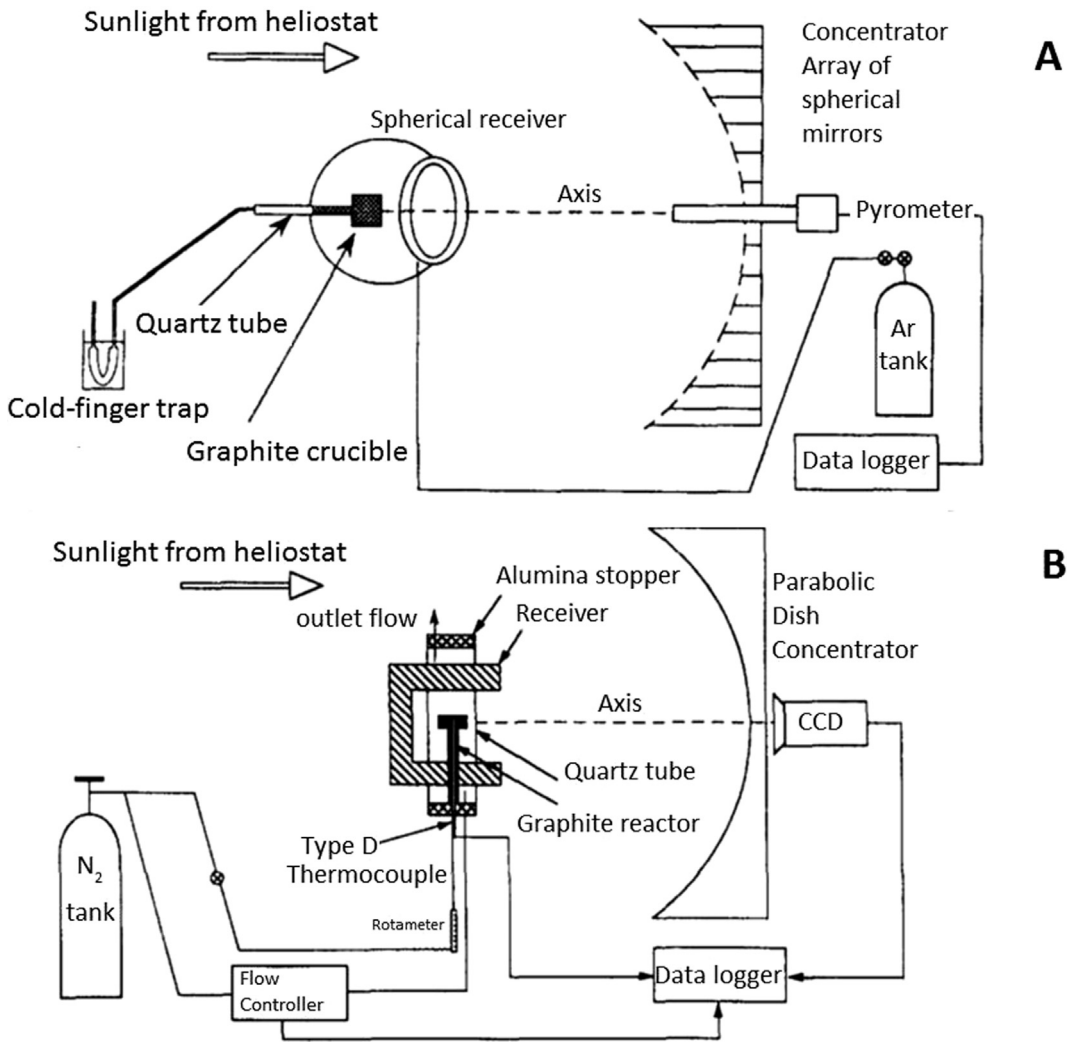

Fig. 9. A) Experimental layout used in the experiments at the University of Minnesota B) Experimental layout used in the experiments at the Paul Scherrer Institute (reprinted from Murray et al. (1995) with permission of Elsevier (Copyright 1995)).

high temperatures and hostile atmospheres. The method of E.G. Acheson (1892) is the typical used in the production of SiC and uses silica sand and coke at high temperatures (1700–2500 °C) (carbothermal reduction of silica). Chemical vapor deposition is other method.

Cruz-Fernandes et al. (1998) studied the possibility of synthetizing SiC in a solar furnace of the Plataforma Solar de Almería. Cruz-Fernandes et al. (1998) used a mixture of silicon (> 99.9% purity) and amorphous carbon (50 μm), in the ratio C/Si = 1.5, with paraffin as binding agent. The mixture was cold pressed at 400 MPa with the purpose of achieving a pellet of 1 cm in diameter and 0.5 cm in height. Cruz-Fernandes et al. (1998) studied the effect of the atmosphere during the tests that consisted in heating up to the maximum temperature in 3 min and holding at that temperature for 30 min. When a 99.9% argon atmosphere (1620 °C maximum temperature) was used, it was possible to obtain 100% SiC, while when a 99.8% N_2 atmosphere was employed, the conversion was not complete as Si_3N_4 appeared. Gulamova et al. (2009) studied the synthesis of silicon carbide in a 1000 kW solar furnace without using protective atmosphere. As initial materials, Gulamova et al. (2009) used quartz (quartzite and quartz sand) and coke, in the ratio C/Si = 2. The power density applied to above samples, loaded into a graphite crucible (30–370 g), was varied between 600 and 790 W/cm^2. With power densities of around 600 W/cm^2 the presence of SiC was not detected, being the reaction products: α-quartz and α-crystobalite, with traces of unreacted carbon. Power densities of 680 W/cm^2 promoted the partial formation of β-SiC. Finally, power densities of 710–780 W/cm^2 allowed reaching the total conversion of the initial material into β-SiC.

Ceballos-Mendivil et al. (2015) synthesized SiC in a solar furnace. They divided the process into five stages where only in the last two, concentrated solar energy was used. The first stage consisted in synthesizing silica by means of the sol-gel process (see Hench and West, 1990 for further information about the sol-gel process). In the second stage, silica was mixed with sucrose, H_2SO_4 and distilled water. The third stage consisted in drying the mixture obtained in stage two. The fourth stage was based on the synthesis of the SiO_2/C nanocomposite. The fifth stage was the obtaining of the SiC. Ceballos-Mendivil et al. (2015) used a solar furnace of 25 kW located in the Instituto of Energías Renovables of the UNAM (México). The synthesis of the composite SiO_2/C was carried out using the reagent obtained in the stage three in a chamber of nitrogen and temperatures of 700 °C for 1 h. In the fifth stage, the SiC (chiefly β-SiC with small amounts of α-SiC) was obtained from the SiO_2/C composite. This process as opposed to those proposed by Cruz-Fernandes et al. (1998) and Gulamova et al. (2009) is not based on powder metallurgy. It follows a complex process that could be useful in the production of SiC to be used as catalytic supports, electronic and photoelectric devices or as reinforcement in composites and materials for high temperature applications. The processes proposed by Cruz-Fernandes et al. (1998) and Gulamova et al. (2009) seems a version of the conventional process where silica sands or high-purity quartz are

mixed with coke and melted in an electric arc furnace at temperatures of around 2000 °C, but in this case, the energy provided by the electric arc furnace is here supplied by concentrated solar energy. In this way, through replacing electric power by solar power, energy costs are supposed to be reduced, the same as the environmental protection derived from the utilization of a renewable energy source. Both Cruz-Fernandes et al. (1998) and Gulamova et al. (2009) obtain similar results, and in a progression in the research in this field, quartz is used as starting material in Gulamova et al. (2009) instead of silicon as in **Cruz-Fernandes et al. (1998)**.

4.2.1.2. Silicon nitride (Si_3N_4). The obtaining of dense ceramics with nanogranulated microstructure is complicated by using conventional techniques because of the fast grain growth rate. Several methods of fast sintering have been developed as microwave sintering, spark plasma sintering and ceramic densification in solar furnace. One of these compounds is the silicon nitride (Si_3N_4), characterized by its high flexural strength, high fracture toughness and creep resistance even at high temperatures, but also by its high thermal shock resistance if compared with most ceramic materials (Cardarelli 2008). From the chemical point of view, silicon nitride exhibits an excellent corrosion resistance to numerous molten nonferrous metals (Al, Pb, Zn, Cd, Bi, Rb and Sn) as well as to molten salts (NaCl-KCl, NaF and silicate glasses) (Cardarelli 2008).

Zhilinska et al. (2003) sintered Si_3N_4 composites from nanometric powders. They carried out tests in the Plataforma Solar de Almería with thermal cycles of 30–180 °C/min heating rate and 10–60 min holding time at maximum temperatures (1600–1750 °C). Zhilinska et al. (2003) prepared two kinds of samples: α/β-SiAlON and Si_3N_4-$6Y_2O_3$-$3Al_2O_3$, by means of plasmachemical synthesis in nitrogen plasma, using metallic (Si, Al) and oxide (Y_2O_3, Al_2O_3) powders as raw materials. It was observed for Si_3N_4-$6Y_2O_3$-$3Al_2O_3$ samples that at 1700 °C of sintering temperature, with fast heating rate (180 °C/min) and 10 min holding time, it was possible to almost reach the theoretical density (94%). Mechanical properties depend on both the density and β-Si_3N_4 phase content, and at 1750 °C the best results of density and the best hardnesses values were reached (independently on the heating rate and holding time) but with acicular β-Si_3N_4. In the case of α/β-SiAlON, sintering happened at lower temperatures (1600 °C, 95% density) with β-SiAlON as present phase with fine grain structure. Zhilinska et al. (2003) observed that results were like those obtained by conventional methods. In this way, concentrated solar energy could be a competitive method for fast sintering, as fast heating and cooling rates can be obtained and thus avoiding the fast grain growth rate.

4.2.2. Alumina

First researches in the synthesis of alumina compounds date from 1990, when Adylov et al. 1990 produced alumina-magnesia spinel-based ceramic in a solar furnace.

Cruz-Fernandes et al. (2000) sintered high alumina powders (99.7% Al_2O_3; $d_{50} = 0.5$ μm) in a solar furnace. Before solar experiments, powders were compacted into discs (12 mm in diameter and 3 mm in thickness) by applying a pressure of 20 MPa at room temperature. Cruz-Fernandes et al. (2000) used the Uzbek Academy of Sciences (Uzbekistan) solar furnace to perform tests, where thermal cycle was: 45 °C/min heating rate, holding time of 30 min at 1600 °C, and 30 °C/min cooling rate. Cruz-Fernandes et al. (2000) compared mechanical strength (through the Modulus of Rupture, MOR) of solar sintered alumina discs with discs sintered by traditional method. They observed that traditionally sintered specimens had a MOR of 166.1 ± 29.2 MPa while solar sintered specimens had a MOR of 131.2 ± 23.5 MPa. Cruz-Fernandes et al. (2000) concluded that internal stresses in the solar sintered discs caused this difference because of the fast heating and cooling rates. This powder metallurgy process could find application in short series parts as other processes described in this section 4. However, the problem of sintering ceramics by using concentrated solar energy is the fast heating and cooling rates that could be achieved. These fast heating and cooling rates can be useful in reducing the time of the processes, but they may be problematic in the case of certain ceramics as a consequence of the internal stresses (in certain ceramic materials, thermal shock resistance might be a problem) and the lack of stress relieving processes typical in metals. For that reason, heating and cooling rates should be controlled and studied in order to avoid the problems of internal stresses.

Román et al. (2008) synthesized alumina powders (α-Al_2O_3) through the route of homogeneous precipitation with urea. These powders were treated until obtaining powders of 60 μm that were *iso*-pressed at 200 MPa to consolidate green compacts. This green product was pre-sintered at 1200 °C for 4 h, and then cut into discs of 15 mm in diameter and 2.5 mm in thickness before solar experiments in the Plataforma Solar de Almería. Román et al. (2008) carried out experiments where heating rate (50–100 °C/min), sintering temperature (1600–1780 °C) and furnace atmosphere (air, argon and 95 N_2-$5H_2$) were controlled. Román et al. (2008) obtained microstructures of a complex alumina matrix (some impurities of SiO_2, CaO, ZrO_2 and MgO were distributed at grain boundaries, triple points, and matrix voids) that gave lower densities than calculated (91–99% of theoretical 3.97 g/cm^3), but higher than in electric furnace (89% of theoretical). That was the reason of that Román et al. (2008) observed that solar sintering favored the densification, but also that fast heating rates and short sintering times during solar treatments restrained grain growth. Román et al. (2008) observed that grain growth was promoted by increasing temperature rather than heating time, but at temperatures above 1780 °C enhanced densification (99%) with partial fusion of samples. Tests under argon atmosphere allowed 98% densification and 50 μm average grain size, while 95 N_2-$5H_2$ allowed 99% densification and 100 μm average grain size, in both cases with 60 min holding time, 1600 °C sintering temperature and 50 °C/min heating rate.

4.2.3. Titanium carbide

Titanium carbide is an extremely hard refractory ceramic material that is used in the manufacture of cutting tools due to its high hardness (9–9.5 in the Mosh scale). The synthesis of this compound by using concentrated solar energy was also studied.

Cruz-Fernandes et al. (1999) studied the interaction between Ti and Zr (M) and C (graphite) or amorphous carbon under argon or N_2 atmosphere in a solar furnace of the Plataforma Solar de Almería, with the idea of obtaining non-stoichiometric carbide MC_X ($0.5 < X < 1$) and carbonitride MC_XN_Y ($0.5 < X + Y < 1$). They used Ti (99% pure, < 45 μm) or Zr (99.7% pure, < 125 μm) powders that were mixed with carbon powders (graphite or amorphous carbon) in mole ratio C/M of 1.5 to make a green compact (10 mm diameter and 5 mm of thickness) by applying pressure (400 MPa). The reaction was carried out under argon atmosphere for preparing MC_X, and under N_2 atmosphere for preparing MC_XN_Y for 30 min at 1600 °C and using concentrated solar energy as energy source. Cruz-Fernandes et al. (1999) carried out carburizing and carbonitriding reactions faster than under the comparable temperature conditions in the traditional laboratory furnace.

Cruz-Fernandes et al. (2002) studied the solar synthetization of hypo-stoichiometric TiC_X (X = 0.50, 0.625, 0.75, 0.85, 0.90 and 1.0). They prepared a green compact (10 mm diameter and 5 mm height) by applying uniaxial pressure of 40 MPa to a mix of Ti (99%; < 45 μm) and graphite powders (< 50 μm) with mole ratio of carbon to titanium of 0.50, 0.625, 0.75, 0.85, 0.90 and 1.0. Experiments were carried out in the Plataforma Solar de Almería under argon atmosphere at 1500 °C for 30 min. After 30 min of exposure, single-phase TiC_x with good crystallinity was obtained. The same as in Cruz-Fernandes et al. (1999) concentrated solar energy is the energy source in this powder metallurgy process. Energetically talking, costs of producing titanium carbide parts could be significantly reduced, however, and although reactions of carburizing and carbonitriding take place faster than in the traditional

laboratory furnace, long series of titanium carbide parts do not seem possible to be obtained by using concentrated solar energy due to the sizes of the parts described in this paper.

4.2.4. Tungsten carbide (WC)

Tungsten carbide is a refractory compound, commonly used due to its good wear resistance conferred by its high hardness (around 9 in the Mosh scale). The manufacture is performed by means of sintering tungsten carbide powders and a certain amount of cobalt.

Guerra-Rosa et al. (2002) studied the WC sintering using Co as additive by preparing cylindrical specimens of 5 mm in diameter and 5 mm in height with WC-10 wt% Co in the form of green powders (powders were compacted by applying uniaxial pressure of around 50 MPa). Thermal treatment cycle was short with no more than 5 min at sintering process temperature (1500 °C). The properties compared with conventionally obtained samples were 14.3 ± 0.3 g/cm^3 (14.5 ± 0.2 g/cm^3 conventional), 13.14 ± 0.96 GPa (12.56 ± 0.11 GPa conventional) and 12.3 ± 1.5 MPa m$^{1/2}$ (14.2 ± 0.8 MPa m$^{1/2}$ conventional). The process proposed by Guerra-Rosa et al. (2002) is based on the powder metallurgy. It could be very useful in the manufacture of parts with wear resistance in short times, with low energy costs and with similar properties if compared with conventional synthesis methods.

Researches described below are based on the synthesis of tungsten carbide and not in powder metallurgy as that proposed by Guerra-Rosa et al. (2002). Dias et al. (2007) obtained WC whiskers by heating C/W mixtures at temperatures of 1900 °C, but not at 1600 °C. These nanometer WC whiskers might be collected and used as acicular reinforcement in metal matrix composites or in tools. Costa-Oliveira et al. (2007) also studied the obtaining of tungsten carbide via concentrated solar energy. W_2C was observed as well as WC when heating up to 1600 °C extremely fast (one of the main characteristics of the processes based on concentrated solar energy), but W_2C did not convert fully to WC even after 30 min at a temperature exceeding 2500 °C in argon atmosphere. Costa-Oliveira et al. (2008) attempted the solar synthesis of W_2C by heating C/W mixtures (between 0.35 and 0.50) up to 1600 °C and 1900 °C under argon atmosphere in a solar furnace. As observed by Shohoji et al. (2010), the synthesis of single phase W_2C was difficult as this phase coexisted with free metallic W. In the upper surface layer of the pellet treated at 1900 °C, nanometer WC whiskers over W_2C grains are observed (as in Dias et al., 2007).

Shohoji et al. (2010) studied heterogeneity along the height in disc specimens of graphite/tungsten. Experiments were carried out in a solar furnace at Plataforma Solar de Almería under argon gas inert atmosphere at 1600 °C by using pellets (10 mm in diameter and 4 mm thickness, compacted by uniaxial pressing at 450 MPa) of graphite/tungsten powder mixtures in C/W atom ratios of 0.35, 0.50 and 1.00. Top surface consisted in WC for any examined specimen, while bottom surface constitution depended on the C/W ratio: C/W = 0.35 exhibited almost pure W; C/W = 0.5 presented mainly W with small amount of W_2C; and, C/W = 1.00 showed W_2C as main phase with small proportion of WC. The phases in the intermediate layer also depended on the C/W ratio: C/W = 0.35 presented coexisting W and W_2C; C/W = 0.50, pure W_2C was observed; and C/W = 1.00 indicated predominant WC with trace W_2C. If homogenous specimen is desired certain extent of the upper and bottom layer should be removed. This process, the same as that proposed by Guerra-Rosa et al. (2002), could be applied in the production of parts with wear resistance through a process competitive in quality.

4.2.5. Tantalum carbide

Tantalum carbides are a family of compounds collected with the formula TaC_x, where × usually varies in the range 0.4–1. These compounds are characterized by being hard, brittle, and refractory (> 3500 °C melting point). The manufacture of these compounds is performed by heating (at about 2000 °C) a mixture of tantalum and graphite of the considered composition in vacuum or argon atmosphere. Alternatively, the carbothermal reduction of tantalum pentoxide in vacuum or hydrogen atmosphere (1500–1700 °C) is carried out. Cruz-Fernandes et al. (2006) studied the solar obtaining of tantalum carbide in a 1.5 kW solar furnace. Experiments were performed at 1600 °C for 30 min. They observed that equilibrium reaction product of Ta with excess carbon (amorphous carbon or graphite) is TaC, with Ta_2C as intermediate reaction product. It is possible to check that temperatures are like those reached by traditional methods, although reaching that temperature by using a renewable energy. Moreover, the process proposed by Cruz-Fernandes et al. (2006) could be economically competitive as the costs of reaching that temperature come from installation costs and not from energy costs.

4.2.6. Molybdenum carbide

Molybdenum carbide (MoC and Mo_2C) is also a hard-refractory ceramic material, which appears in steels when alloyed with molybdenum (corrosion resistance as well as hardness are increased in presence of this phase (Pero-Sanz et al., 2017)). Other applications of molybdenum carbide include cutting tools and parts manufactured through powder metallurgy technique (with wear resistance). However, the interest of molybdenum carbide is found as catalyst for photocatalytic H_2 evolution from water (Wang et al., 2016; **Ma et al., 2017**). Shohoji et al. (2007) studied the formation of η-MoC_{1-x} by using concentrated solar energy. They prepared compacted pellets (12 mm in diameter and 5 mm in height compacted by applying uni-axial pressure of 400 MPa) of Mo and graphite powder (C/Mo atom ratio = 1.5/1) that were heated up to 1600 °C. η-MoC and Mo_2C in presence of excess of free carbon were detected after 90 min holding time at 1600 °C. Granier et al. (2008) studied the synthesis of molybdenum carbide at 1900 °C, considering compacted powder mixtures of graphite and molybdenum in the C/Mo mole ratios of 2/3, 3/4, 1/2 and 1/1. The formation of β-Mo_2C was observed for any chosen C/Mo, while certain proportion of η-MoC_{1-x} (apart from β-Mo_2C) was observed for the mole ratios 2/3 and 3/4. Granier et al. (2009) performed similar experiments at 1600 °C and exceeding 2500 °C. η-MoC_{1-x} and β-Mo_2C were detected depending on both the C/Mo ratio and the temperature. The synthesis of molybdenum carbide via concentrated solar energy could be competitive with traditional processes (as those based on direct carbonization of metals with graphitic carbon at high temperature, Wang et al. (2007)) or modern methods (as chemical vapor deposition, Nagai et al. (2000); or those that use lasers, Lightstone et al. (2003)).

5. Solar energy in fullerenes and carbon nanotubes

A fullerene is a molecule formed by carbon that adopts the form of a soccer ball. Since the moment when fullerenes were discovered, they became in a topic of interest in science because of their chemical and physical properties, which could make them usable in nanotechnology.

Fullerenes were observed for the first time in 1985 (Amer, 2010) and synthesized in 1989 (Hale et al., 1994). They have many applications in advanced materials that include semiconductors, superconductors, metals of high performance and medical applications. Fullerenes are manufactured by means of graphite vaporization, pulsed laser, resistive heating, and arc of carbon, but none of them can produce fullerenes in economic quantities. All these methods require a source of carbon clusters in gaseous phase. There are two methods: by hydrocarbons combustion (such as benzene in a flame with low oxygen) it is possible to achieve high percentage of fullerenes in the soot, but the rate of fullerenes compared with the mass of hydrocarbons consumed is low; and, by vaporization of elemental carbon at temperatures up to 3000 °C. This material was very popular between the late 1980 s and early 2000 s, and it was a very important field of research and development (especially due to the potential medical applications). However, Andre Geim and Konstantin Novoselov rediscovered, isolated, and characterized the graphene in 2004, and this “new” material became in

Table 4
Evolution in the synthesis of fullerenes by using concentrated solar energy.

Date	Quantity	Reference
Early 90 s	< Tens of milligrams	Chibante et al. (1993); Fields et al. (1993) and Hale et al. (1994)
Medium 90 s	80–200 mg/h	Laplaze et al. (1996)
Early 2000 s	80–150 g/h carbon soot	Flamant et al. 2004a and Flamant et al. (2004b)

a very popular material because of the potential applications mainly in electronics. The appearance of graphene relegated fullerenes to a second plane. The evolution in the obtaining of fullerenes by using concentrated solar energy is showed in Table 4.

First experiences regarding both concentrated solar energy and fullerenes date from the early 1990 s. Chibante et al., (1993); Fields et al. (1993) and Hale et al. (1994) studied the synthesis of fullerenes in a solar furnace. They could synthesize fullerene quantities of no more than tens of milligrams. Laplaze et al. (1996) studied the effects of pressure (50–350 hPa) and gas flow (0.2–0.7 sm^3/h) in fullerene yield, and they could synthesize fullerene quantities of around hundreds of milligrams (80–200 mg/h). Regarding to the fullerene yield, Laplaze et al. (1996) observed the best results (10% yield) when using argon (better than helium), pressures of 70 hPa and gas flow of 0.5 sm^3/h. The final results in fullerene researches are from the early 2000 s, after several previous studies (Guillard et al. (2001a) and Guillard et al. (2001b) studied the reactors conditions for the synthesis of fullerenes and carbon nanotubes), Flamant et al. (2004a) obtained quantities of grams by using a 50 kW solar furnace (see Fig. 10). The same as Laplaze et al., 1996; Flamant et al. 2004a studied the role of pressure and gas flow on fullerenes rate, observing the best results (13.5% yield) when using helium at 450 hPa and 10 sm^3/h. Flamant et al. (2004b) proposed a solar reactor for graphite vaporization in the fullerene synthesis (80–150 g/h carbon soot). The technology of fullerenes production is well studied to produce significant quantities of this material. However, the relegation of fullerenes to a second plane in research has led to the almost inexistence of applications for this material.

Carbon nanotubes were discovered in the early nineties and can be designed as carbon allotropes with cylindrical nanostructure. Their properties give them several possible applications in coatings and films, microelectronics, energy storage and biotechnology (de Volder et al., 2013). Luxembourg et al. (2005) synthesized single-walled carbon nanotubes in gram quantities in a 50 kW solar reactor (10–15 g/h single-wall carbon nanotube's rich soot, Flamant et al., 2005). Luxembourg et al. (2005) obtained 1.2–1.6 nm in diameter carbon nanotubes with helium buffer gas at 450 hPa, 8 Nm^3/h and a 15 cm target length using 2 at.% Ni and 2 at.% Co as catalyst.

Concentrated solar energy could be a high-energy source competitive with lasers and other techniques in the field of carbon structure compounds synthesis (in quantities of carbon structures obtained but also economically). The problem is that nowadays fullerenes and nanotubes have been relegated to a second plane as a consequence of the growing interest in graphene applications.

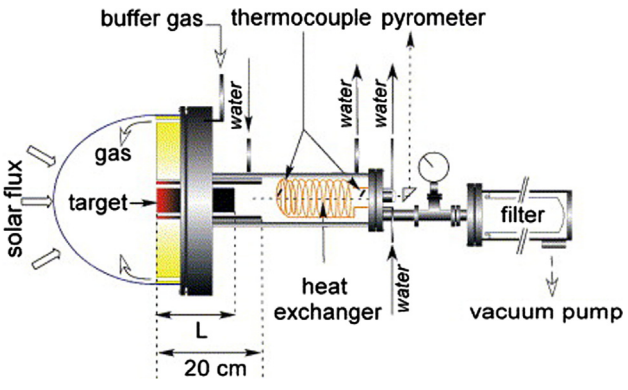

Fig. 10. Scheme of the set up used in the experiments at Odeillo (reprinted from Flamant et al. (2004a) with permission of Elsevier (Copyright 2004)).

6. Solar energy in the production of lime

The production of lime is one of the few processes where concentrated solar energy is involved that was studied since the economical point of view. Lime is mainly used in the production of cement, but also in cosmetics and pharmaceuticals. The solar process for the lime obtaining was studied by Flamant et al. (1980); Imhof (1997); Meier et al. (2004) and Meier et al. (2006). The energy required for the limestone calcination is calculated according to the following chemical reaction:

$$CaCO_3(s) \rightarrow CaO(s) + CO_2$$

in 3029 kJ/kg CaO at the decomposition temperature (1173 K). In modern kiln furnaces this value ranges among 3600 kJ/kg CaO for vertical double shaft kilns and 7500 kJ/kg CaO for non-preheated long rotary kilns. Similar experiments were conducted by Salman (1988) as he studied the thermal decomposition of limestone and gypsum and obtained maximum conversions of 65% and 38%, respectively.

Meier et al. (2004; 2005a) and Meier et al. (2006) designed a kiln furnace heated indirectly by means of a system of rotatory tubes (see Fig. 11). Absorber tubes were heated by means of solar energy and were responsible of heating the load. Meier et al. (2006) used a 15 kW solar furnace. 1.5–2 h were required until stationary conditions were reached, after that the treatment lasted 30 min (1200–1400 K), with rotation speeds between 8 and 18 rpm, being the feeding rate of 36–136 g/min and particle size between 2 and 3 mm. Meier et al. (2006) observed a calcination rate of 98.2% and CaO productivity of 64.2 g/min when the temperature was 1395 K.

Meier et al. (2005b) studied the possible advantages and disadvantages of using concentrated solar energy in the production of lime. They observed a reduction of CO_2 emissions by 20% in a state-of-the-art lime plant and up to 40% in a conventional cement plant. Meier et al. (2005b) observed that for a solar calcination plant with 25 MW_{th}, the cost of solar produced lime ranged between 128 and 157 $/ton (2004), which was twice the selling price of conventional lime in 2004. Meier et al. (2005b) suggested that the field of solar production of high purity lime could be the chemical and pharmaceutical sectors. It is clearly observed that concentrated solar energy process for the lime production was not competitive with conventional methods (at least according to Meier's et al. calculations), at least if we consider the cement industry. As other processes described throughout this paper, this solar technology should focus on high added value industries, as are the cases proposed by Meier et al. (2005b): pharmaceutical and chemical sectors. Other problem, that should be considered in the solar lime is

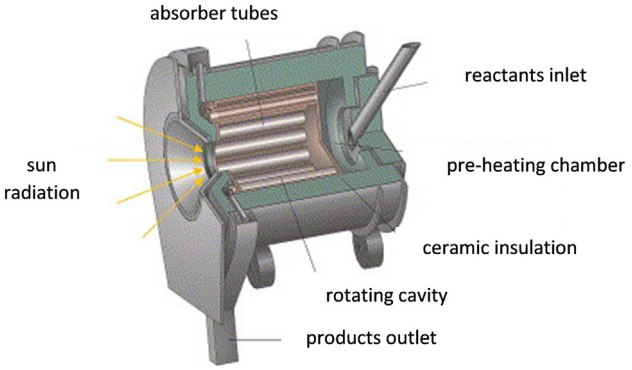

Fig. 11. Schematic representation of the multi-tube rotary kiln solar furnace prototype (reprinted from Meier et al. (2006) with permission of Elsevier (Copyright 2006)).

that cement plants are usually located near to consumers (or harbors), to sources of limestone and sometimes near to steel factories that provide certain raw materials (blast furnace slag), and in that places sun conditions are not always those required to ensure the competitiveness of solar process.

7. Conclusions

Solar energy offers a great potential in applications of high temperature. As opposed to conventional processes used in metallurgy, materials processing, and non-metallic materials, concentrated solar energy has costs that are not dependent on the temperature (in conventional processes, the higher the temperature, the higher the energy consumption), and in this way, could compete with modern technologies, including laser or plasma.

As opposed to other renewable energy sources, such as biofuels or biomass that could be used in the generation of heat for reaching the high temperatures required in the metallic and non-metallic industries, solar energy generates neither CO_2 nor other polluting agents. In this way, both greenhouse effect and atmosphere contamination would be reduced.

The main drawback of solar energy is the impossibility of working 24 h per day because of the sun availability. This question limits the applications in metallurgy, as zinc, aluminum, steel are produced in quantities that require plants operating 24 h 365 days yearly. In the field of metallurgy, concentrated solar energy could find application in the recovery of wastes coming from metallurgical processes, as is the case of the mill scale treated in a fluidized bed heated with concentrated solar energy. The same as in metallurgy happens in the processing of materials or in the manufacture of ceramics, as concentrated solar energy has no interest in applications where important quantities of materials are considered. Concentrated solar energy could find applications in short series of products (as for instance in obtaining of hard refractory ceramics), high purity materials (as for instance the production of lime for the chemical and pharmaceutical industries) or in materials recently discovered (as for instance fullerenes and carbon nanotubes). The most promising process of those described in this paper is the couple Zn/solar energy for energy storage (and also the unique with a long temporary line, from early eighties until nowadays), where pilot-plat studies have been carried out, and could be applied at an industrial scale in the future.

Acknowledgements

This research was supported by the Spanish Ministry of Education, Culture, and Sports via an FPU (Formación del Profesorado Universitario) grant to Daniel Fernández González (FPU014/02436).

ReferencesReferences introduction

Charpentier, L., Dawi, K., Eck, J., Pierrat, B., Sans, J., Balat-Pichelin, M., 2011. Concentrated solar energy to study high temperature materials for space and energy. J. Solar Energy Eng. 133 (3), 031005–031013.

D'Elia, R., Bernhart, G., Cutard, T., Perandan, G., Balat-Pichelin, M., 2014. Preliminary test of silicon carbide based concretes for hybrid rocket nozzles in a solar furnace. Acta Astronautica 99, 242–251.

Eglinton, T., Hinkley, J., Beath, A., Dell'Amico, M., 2013. Potencial applications of concentrated solar thermal technologies in the Australian minerals processing and extractive metallurgical industry. JOM 65 (12), 1710–1720.

Farber, E.A., 1964. Crystals of high-temperature materials produced in the solar furnace. Solar Energy 8 (1), 38–42.

Flamant, G., Ferriere, A., Laplaze, D., Monty, D., 1999. Solar processing of materials: Opportunities and new frontiers. Solar Energy 66 (2), 117–132.

Flamant, G. and Balat-Pichelin, M., 2010, Elaboration and testing of materials using concentrated solar energy, in Solar Energy Conversion and Photoenergy Systems. Thermal Systems and Desalination Plants. Volume I. In: Blanco Gálvez, J., Rodríguez, S.M., Delyannis, E., Belessiotis, V.G., Bhattacharya, S.C., Kumar, S. (Eds.), Encyclopedia of Life Support Systems. United Kingdom: Eolss Publishers Co., Ltd./UNESCO, pp. 363–389.

Gosh, G.K., 1991. Solar Energy, The Infinite Source. APH Publishing Corporation, New Delhi.

Herranz, G. and Rodríguez, G. P., 2010, Uses of Concentrated Solar Energy in Materials Science, Chapter 8 in Solar EnergyIn: Rugescu, R.D. (Ed.), InTech, pp. 145–170.

Konstandopoulos, A. G., Pagkoura, C., and Lorentzou, S., 2012, Solar fuels and industrial chemistry, in Concentrating Solar Power Technology: Principles, Developments and Applications. In: Lovegrove, K., Stein, W. (Eds.), Cambridge: Woodhead Publishing Limited, pp. 620–654.

Kovacik, J., Emmer, S., Rodríguez, J., Cañadas, I., 2014. Solar Furnace: Thermal Shock Behaviour of TiB_2 Coating on Steel, METAL 2014, May 21st-23rd. Czech Republic, Brno.

Martínez, D., Rodríguez, J., 1998. Tratamiento superficial de materiales mediante luz solar concentrada: una opción mediante energías renovables. Revista de Metalurgia de Madrid 34 (2), 104–108.

Martínez, D., Cañadas, I., Mallol, G., Téllez, F., Rodríguez, J., 2015. A case study of the feasibility of using solar concentrating technologies for manufacturing ceramics. J. Clean. Prod. 87, 977–991.

McDonald, D., Hunt, L.B., 1982. A History of Platinum and its Allied Metals, Hatton Garden, London: Ed. Johnson Matthey.

Newcomb, S., 2009. The World in a Crucible: Laboratory Practice and Geological Theory at the Beginning of Geology. The Geological Society of America Inc, Boulder, Colorado.

Revuelta-Acosta, J.D., García-Díaz, A., Soto-Zarazua, G.M., Rico-García, E., 2010. Adobe as sustainable material: A thermal performance. J. Appl. Sci. 10 (19), 2211–2216.

Rodríguez, M.A., Soroza, B., 2006. Determination of the optimum composition of adobe brick for a school in Cuba. Materiales de Construcción 56 (282), 53–62.

Rossi, C., 2010, Archimedes' cannons against the roman fleet?, in The Genius of Archimedes-23 Centuries of Influence on Mathematics, Science and Engineering, Proceedings of an International Conference held at Syracuse, Italy, June 8–10, 2010 (editors Stephanos A. Paipetis, Marco Ceccarelli), London: Springer, pp. 113–132.

Tetsuo, N., Masao, M., and Choji, N., 1957, High temperature research in a solar furnace. I. On the fusion of metal oxides, Bulletin of Reports of the Government Research Institute of Nagoya, 6(11), p. 663.

Tetsuo, N., Masao, M., and Choji, N., 1959, High temperature research in a solar furnace. II. On the fusion of metal oxides, Bulletin of Reports of the Government Research Institute of Nagoya, 8(1), p. 61–67.

Van den Abeelen, L., 2017. Spaceplane HERMES: Europe's Dream of Independent Manned Spaceflight, 1st edition. Springer Praxis Books, Hilversum, The Netherlands.

Venn, F., 2002, The Oil Crisis, New York, NY: Ed. Taylor and Francis.

References metallurgy

Abanades, S., Charvin, P., Flamant, G., 2007. Design and simulation of a solar chemical reactor for the thermal reduction of metal oxides: Case study of zinc oxide dissociation. Chem. Eng. Sci. 62 (22), 6323–6333.

Adinberg, A., Epstein, M., 2004. Experimental study of solar reactors for carboreduction of zinc oxide. Energy 29, 757–769.

Brkic, M., Koepf, E., Meier, A., 2016. Continuous solar carbothermal reduction of aerosolized ZnO particles under vacuum in a directly irradiated vertical-tube reactor. J. Solar Energy Eng. 138 (2), 021010–021024.

Brkic, M., 2017, Solar-Driven Vacuum Carbothermal Reduction of Zinc Oxide in a Drop-Tube Reactor, Doctoral Thesis, ETH Zurich.

Chambon, M., Abanades, S., Flamant, G., 2010. Design of a lab-scale rotary cavity-type solar reactor for continuous thermal dissociation of volatile oxides under reduced pressure. J. Solar Energy Eng. 132 (2), 021006–021013.

Chambon, M., Abanades, S., Flamant, G., 2011. Thermal dissociation of compressed ZnO and SnO_2 powders in a moving-front solar thermochemical reactor. AlChE J. 57 (8), 2264–2273.

Epstein, M., Yogev, A., Yao, C., Berman, A., 2001. Carbothermal reduction of alkali hydroxides using concentrated solar energy. Energy 26, 441–455.

Epstein, M., Ehrensberger, K., Yogev, A., 2004. Ferro-reduction of ZnO using concentrated solar energy. Energy 29, 745–756.

Epstein, M., Olalde, G., Santén, S., Steinfeld, A., Wieckert, C., 2008. Towards the industrial solar carbothermal production of zinc. J. Solar Energy Eng. 130, 014501–014504.

Fernández, D., Ordiales, M., Sancho, J., and Verdeja, L. F., 2015, Posibilidades de la lógica difusa en operaciones y procesos de la metalurgia primaria, Spain Minergy Congress 2015, Gijón/Xixón, Asturias, Spain, 15–19 June 2015.

Fernández-González, D., Martín-Duarte, R., Ruiz-Bustinza, I., Mochón, J., González-Gasca, C., Verdeja, L.F., 2016. Optimization of sínter plant operating conditions using advanced multivariate statistics: Intelligent data processing. JOM 68 (8), 2089–2095.

Fernández-González, D., Ruiz-Bustinza, I., Mochón, J., González-Gasca, C., Verdeja, L.F., 2017a. Iron ore sintering: Raw materials and granulation. Min. Process. Extract. Metall. Rev. 38 (1), 36–46.

Fernández-González, D., Ruiz-Bustinza, I., Mochón, J., González-Gasca, C., Verdeja, L.F., 2017b. Iron ore sintering: Process. Min. Process. Extract. Metall. Rev. 38 (4), 215–227.

Fernández-González, D., Ruiz-Bustinza, I., Mochón, J., González-Gasca, C., Verdeja, L.F., 2017c. Iron ore sintering: Quality indices. Min. Process. Extract. Metall. Rev. 38 (4), 254–264.

Fernández-González, D., Ruiz-Bustinza, I., Mochón, J., González-Gasca, C., Verdeja, L.F., 2017d. Iron ore sintering: Environment, automatic and control techniques. Min. Process. Extract. Metall. Rev. 38 (4), 238–249.

Fernández-González, D., Piñuela-Noval, J., and Verdeja, L. F., 2018, Iron ore agglomeration technologies, in Iron Ores and Iron Oxide Materials (edited by Volodymyr Shatokha), Intech (ISBN: 978-953-51-5824-0).

Flamant, G., Kurtcuoglu, V., Murray, J., Steinfeld, 2006. Purification of metallurgical grade silicon by a solar process. Solar Energy Mater. Solar Cells 90, 2099–2106.
Fletcher, E.A., Noring, J.E., 1983. High temperature solar electrothermal processing- Zinc from zinc oxide. Energy 8, 247–254.
Fletcher, E.A., Macdonald, F.J., Kunnerth, D., 1985. High temperature solar electro-thermal processing-II. Zinc from zinc oxide. Energy 10, 1255–1272.
Hauter, P., Moeller, S., Palumbo, R., Steinfeld, A., 1999. The production of zinc by thermal dissociation of zinc oxide-solar chemical reactor design. Solar Energy 67 (1–3), 161–167.
Koepf, E., Advani, S.G., Steinfeld, A., Prasad, A.K., 2012. A novel beam-down, gravity-fed, solar thermochemical receiver/reactor for direct solid particle decomposition: Design, modelling, and experimentation. Int. J. Hydrogen Energy 37 (22), 16871–16887.
Koepft, E.E., Advani, S.G., Prasad, A.K., Steinfeld, A., 2015. Experimental investigation of the carbothermal reduction of ZnO using a beam-down, gravity-fed solar reactor. Indus. Eng. Chem. Res. 54 (33), 8319–8332.
Koepft, E., Villasmil, W., Meier, A., 2016. Pilot-scale solar reactor operation and characterization for fuel production via the Zn/ZnO thermochemical cycle. Appl. Energy 165, 1004–1023.
Kruesi, M., Galvez, M.E., Halmann, M., Steinfeld, A., 2011. Solar aluminum production by vacuum carbothermal reduction of alumina- Thermodynamic and experimental analyses. Metall. Mater. Trans. B 42B, 254–260.
Levêque, G., Abanades, S., 2013. Kinetic analysis if high-temperature solid-gas reactions by an inverse method applied to ZnO and SnO_2 solar thermal dissociation. Chem. Eng. J. 217, 139–143.
Levêque, G., Abanades, S., 2015. Investigation of thermal and carbothermal reduction of volatile oxides (ZnO, SnO_2, GeO_2 and MgO) via solar-driven vacuum thermo-gravimetry for thermochemical production of solar fuels. Thermochimica Acta 605 (10), 86–94.
Loutzenhiser, P.G., Tuerk, O., Steinfeld, A., 2010. Production of Si by vacuum carbothermal reduction of SiO_2 using concentrated solar energy. JOM 62, 49–54.
Lytvynenko, Y.M., 2013. Obtaining aluminum by the electrolysis with the solar radiation using. Appl. Solar Energy 49 (1), 4–6.
Mochón, J., Ruiz-Bustinza, I., Vázquez, A., Fernández, D., Ayala, J.M., Barbés, M.F., Verdeja, L.F., 2014. Transformations in the Iron-Manganese-Oxygen-Carbon system resulted from treatment of solar energy with high concentration. Steel Res. Int. 85, 1469–1476.
Müller, R., Haeberling, P., Palumbo, R.D., 2006. Further advances toward the development of a direct heating solar thermal chemical reactor for the thermal dissociation of ZnO(s). Solar Energy 80 (5), 500–511.
Murray, J.P., 1999a. Aluminum production using high-temperature solar process heat. Solar Energy 66 (2), 133–142.
Murray, J.P., 1999b, Aluminum-silicon carbothermal reduction using high-temperature solar process heat, 128th TMS Annual Meeting, San Diego, CA, 28 February-4 March, pp. 399–405.
Murray, J.P., 2001. Solar production of aluminum by direct reduction: Preliminary results for two processes. J. Solar Energy Eng. 123, 125–132.
Murray, J.P., Flamant, G., Roos, C.J., 2006. Silicon and solar-grade silicon production by solar dissociation of Si_3N_4. Solar Energy 80, 1349–1354.
Osinga, T., Frommherz, U., Steinfeld, A., Wieckert, C., 2004a. Experimental investigation of the solar carbothermic reduction of ZnO using a two cavity solar reactor. J. Solar Energy Eng. 126, 633–637.
Osinga, T., Olalde, G., Steinfeld, A., 2004b. Solar carbothermal reduction of ZnO: shrinking packed-bed reactor modeling and experimental validation. Indus. Eng. Chem. Res. 43 (25), 7981–7988.
Palumbo, R.D., Fletcher, E.A., 1988. High temperature solar electrothermal processing-III. Zinc from zinc oxide at 1200–1675 K using a non-consumable anode. Energy 13, 319–332.
Perkins, C., Lichty, P.R., Weimer, A.W., 2008. Thermal ZnO dissociation in a rapid aerosol reactor as part of a solar hydrogen production cycle. Int. J. Hydrogen Energy 33 (2), 499–510.
Ruiz-Bustinza, I., Cañadas, I., Rodríguez, J., Mochón, J., Verdeja, L.F., García-Carcedo, F., Vázquez, A., 2013. Magnetite production from steel wastes with concentrated solar energy. Steel Res. Int. 84, 207–217.
Sancho, J., Verdeja, L.F., Ballester, A., 2000. Metalurgia Extractiva. Volumen II. Procesos de Obtención, Madrid: Ed. Síntesis.
Schunk, L.O., Haeberling, P., Wepf, S., Wuillemin, D., Meier, A., Steinfeld, A., 2008. A receiver-reactor for the solar thermal dissociation of zinc oxide. J. Solar Energy Eng. 130 (2), 21009–21015.
Schunk, L.O., Lipinski, W., Steinfeld, A., 2009a. Ablative heat transfer in a shrinking packed-bed of ZnO undergoing solar thermal dissociation. Am. Inst. Chem Eng. 55 (7), 1659–1666.
Schunk, L.O., Lipinski, W., Steinfeld, A., 2009b. Heat transfer model of a solar receiver-reactor for the thermal dissociation of ZnO-Experimental validation at 10 kW and scale-up to 1 MW. Chem. Eng. J. 150 (2–3), 502–508.
Sibieude, F., Ducarroir, M., Tofighi, A., Ambriz, J., 1982. High temperature experiments with a solar furnace: The decomposition of Fe_3O_4, Mn_3O_4, CdO. Int. J. Hydrogen Energy 7, 79–88.
Steinfeld, A., Fletcher, E.A., 1991. Theoretical and experimental investigation of the carbothermic reduction of Fe_2O_3 using solar energy. Energy 16, 1011–1019.
Steinfeld, A., Kuhn, P., Karni, J., 1993. High-temperature solar thermochemistry: Production of iron and synthesis gas by Fe_3O_4-reduction with methane. Energy 18 (3), 239–249.
Steinfeld, A., Brack, M., Meier, A., Weidenkaff, A., Wuillemin, D., 1998. A solar chemical reactor for co-production of zinc and synthesis gas. Energy 23, 803–814.
Tzouganatos, N., Matter, R., Wieckert, C., Antrekowitsch, J., Gamroth, M., Steinfeld, A., 2013. Thermal recycling of Waelsz oxide using concentrated solar energy. JOM 65 (12), 1733–1743.
Villasmil, W., Brkic, M., Wuillemin, D., Meier, A., Steinfeld, A., 2013. Pilot scale demonstration of a 100-kWth solar thermochemical plant for the thermal dissociation of ZnO. J. Solar Energy Eng. 136 (1), 011016–011027.
Vishnevetsky, I., Epstein, M., Ben-Zvi, R., Rubin, R., 2006. Feasibility study on non-windowed solar reactor: ZnO carboreduction as an example. Solar Energy 80, 1363–1375.
Vishnevetsky, I., Ben-Zvi, R., Epstein, M., Barak, S., Rubin, R., 2013. Solar carboreduction of alumina under vacuum. JOM 65, 1721–1732.
Vishnevetsky, I., Epstein, M., 2015. Solar carbothermic reduction of alumina, magnesia and boria under vacuum. Solar Energy 111, 236–251.
Wieckert, C., Palumbo, R., Frommherz, U., 2004. A two-cavity reactor for solar chemical processes: heat transfer model and application to carbothermic reduction of ZnO. Energy 29, 771–787.
Wieckert, C., Frommherz, U., Kräupl, S., Guillot, E., Olalde, G., Epstein, M., Santén, S., Osinga, T., Steinfeld, A., 2006. A 300kW solar chemical pilot plant for the carbothermic production of zinc. J. Solar Energy Eng. 129 (2), 190–196.

References materials processing:

Alexander, B.H., Balluggi, R.W., 1957. The mechanism of sintering in copper. Acta Mater 5, 666–677.
Apostol, I., Mahajan, A., Monty, C.J.A., Saravanan, K.V., 2015. Nanostructured MgTiO3 thick films obtained by electrophoretic deposition from nanopowders prepared by solar PVD. Appl. Surf. Sci. 358 (Part B), 641–646.
Apostol, I., Rodríguez, J., Cañadas, I., Galindo, J., Lanceros Méndez, S., de Abreu, Libanio, Martins, P., Cunha, L., Venkata Saravanan, K., 2018. Concentrated solar energy used for sintering magnesium titanates for electronic applications. Appl. Surf. Sci. 438, 59–65.
Armas, B., Combescure, C., Trombe, F., 1976. Chemical vapor deposition of NbB_2 and TaB_2 through heating by concentration of solar radiation. J. Electrochem. Soc. 123 (2), 308–310.
Arnaud, C., Lecouturier, F., Mesguich, D., Ferreira, N., Chevallier, G., Estournès, C., Weibel, A., Peigney, A., Laurent, C., 2016. High strength-high conductivity nanostructured copper wires prepared by spark plasma sintering and room-temperature severe plastic deformation. Mater. Sci. Eng.: A 649 (1), 209–213.
Besra, L., Liu, M., 2007. A review on fundamentals and applications of electrophoretic deposition (EPD). Progr. Mater. Sciencek 52 (1), 1–61.
Cañadas, I., Martínez, D., Rodríguez, J., Gallardo, J.M., 2005. Viabilidad del uso de la radiación solar concentrada al proceso de sinterización de cobre. Revista de Metalurgia de Madrid, Extr. 165–169.
Fernández, B.J., López, V., Vázquez, A.J., Martínez, D., 1998. Cladding of Ni superalloy powders on AISI 4140 steel with concentrated solar energy. Solar Energy Mater. Solar Cells 53, 153–161.
Ferriere, A., Faillat, G., Galasso, S., Barrallier, L., Masse, J.E., 1999. Surface hardening of steel using highly concentrated solar energy process. J. Solar Energy Eng.-Transactions of the ASME 121, 36–39.
Ferreire, A., Sánchez-Bautista, C., Rodríguez, G.P., Vázquez, A.J., 2006. Corrosion resistance of stainless steel coatings elaborated by solar cladding process. Solar Energy 80, 1338–1343.
García-Cambronero, L. E., Ruíz-Román, J. M., Cañadas, I. and Martínez, D., 2004, Características de la estructura celular en espumas de Al-7Si con mármol obtenidas mediante energía solar concentrada, Proceedings of the IX Congreso Nacional de Materiales, Vigo, Spain, pp. 499–502.
García-Cambronero, L.E., Cañadas, I., Díaz, J.J., Ruíz-Román, J.M., Martínez, D., 2008. Tratamiento térmico de espumación de precursores de aluminio-silicio en horno solar de lecho fluidificado, Proceedings of the X Congreso Nacional de Materiales, San Sebastián, Spain, pp. 261–264.
García-Cambronero, L.E., Cañadas, I., Martínez, D., Ruíz-Román, J.M., 2010. Foaming of aluminium-silicon alloy using concentrated solar energy. Solar Energy 84, 879–887.
García-Cambronero, L.E., Cañadas, I., Ruiz-Román, J.M., Cisneros, M., Corpas-Iglesias, F.A., 2014. Weld structure of joined aluminum foams with concentrated solar energy. J. Mater. Process. Technol. 214, 2637–2643.
García, I., Sánchez-Olías, J., de Damborenea, J.J., Vázquez, A.J., 1998. Síntesis de nitruro de titanio mediante láser y energía solar concentrada. Revista de Metalurgia de Madrid 34, 109–113.
García, I., Sánchez-Olías, J., Vázquez, A. J., 1999. A new method for materials synthesis: Solar energy concentrated by Fresnel lens, Journal of Physic IV France, Proceedings of the 9th Solar PACES International Symposium on Solar Thermal Concentrating Technologies, 9 (PR3), pp. 435–440.
García, I., Gracia-Escosa, E., Bayod, M., Conde, A., Arenas, M.A., Damborenea, J., Romero, A., Rodríguez, G., 2016a. Sustainable production of titanium foams for biomedical applications by concentrated solar energy. Mater. Lett. 185, 420–423.
García, C., Romero, A., Herranz, G., Blanco, Y., Martin, F., 2016b. Effect of vanadium carbide on dry sliding wear behavior of powder metallurgy AISI M2 high speed steel processed by concentrated solar energy. Mater. Charact. 121, 175–186.
Gopalakrishna, K.R., Seshan, S., 1984. Solar furnace for small scale metallurgical applications. In: Curtis, F.A. (Ed.), Energy Developments: New Forms, Renewables, Conservation Ontario, Canada: Ed. Pergamon Press, pp. 585–593.
Gutiérrez-López, J., Levenfeld, B., Várez, A., Cañadas, I., Rodríguez, J., 2010. Solar sintering of Ni-Zn ferrites: Densification and magnetic properties, PM2010 World Congress-Alternative Sintering Processes. Firenze (Italy) 230–237.
Gutiérrez-Vázquez, J.A., Oñoro, J., 2008. Espumas de aluminio. Fabricación, propiedades y aplicaciones,. Revista de Metalurgia 44, 457–476.

Herranz, G., Romero, A., de Castro, V., Rodríguez, G.P., 2013. Development of high speed steel sintered using concentrated solar energy. J. Mater. Process. Technol. 213, 2065–2073.
Herranz, G., Romero, A., de Castro, V., Rodríguez, G.P., 2014. Processing of AISI M2 high speed steel reinforced with vanadium carbide by solar sintering. Mater. Des. 54, 934–946.
Kaddou, A.K., Abdul-Latif, A., 1969. The feasibility of joining metal using a solar furnace. Solar Energy 12, 377–378.
Karalis, D.G., Pantelis, D.I., Papazo, 2005. On the investigation of 7075 aluminum alloy welding using concentrated solar energy. Solar Energy Mater. Solar Cells 86, 145–163.
Karalis, D.G., Pantelis, D.I., Daniolos, N.M., Bougiouri, V.D., Rodríguez, J., Karakizis, P. N., Kazasidis, M.E., 2017. An attempt of 5083–H111 aluminum alloy welding using variable concentrated solar energy, 6th ICMEN International Conference Tessaloniki, Greece.
Kim, I.S., Prasad, Y.K.D.V., Stoynov, L.A., 2004. A study on an intelligent system to predict the tensile stress in welding using solar energy concentration. J. Mater. Process. Technol. 153–154, 649–653.
Kovacik, J., Emmer, S., Rodríguez, J., Cañadas, I., 2017. Sintering of HDH Ti poder in a solar furnace at Plataforma Solar de Almería. J. Alloys Compd. 695, 52–59.
Lacasa, D., Berenguel, M., Yebra, L., Martínez, D., 2006. Copper sintering in a solar furnace through fuzzy control. In: Proceedings of the 2006 IEEE, International Conference on Control Applications, Munich, Germany, October 4–6, 2006, pp. 2144–2149.
Llorente, J., Vázquez, A.J., 2009. Solar hardening of steel with a new scale solar concentrator. Mater. Chem. Phys. 118, 86–92.
Maiboroda, V.P., Pasichnyi, V.V., Palaguta, N.G., Stegnii, A.I., Krivenko, V.G., 1986. Special features of local heat treatment of steel 34KhN3MFA in the focal spot of a solar furnace. Metal Sci. Heat Treat. 28, 78–80.
Pantelis, D.I., Griniari, A., Sarafoglou, Ch., 2005. Surface alloying of pre-deposited molybdenum- based powder on 304L stainless steel using concentrated solar energy. Solar Energy Mater. Solar Cells 89, 1–11.
Pantelis, D.I., Karakizis, P.N., Kazasidis, M.E., Karalis, D.G., Rodríguez, J., 2017. Experimental and numerical investigation f AA6082-T6 thin plates welding using concentrated solar energy (CSE). Solar Energy Mater. Solar Cells 171, 187–196.
Pero-Sanz, J.A., 2004. Aceros. Metalurgia Física, Selección Y Diseño. CIE Inversiones Editorial Dossat, Madrid.
Pero-Sanz, J.A., Fernández-González, D., Verdeja, L.F., 2018. Materiales Para Ingeniería. Pedeca Press Publicaciones S. L. U, Fundiciones Férreas, Madrid.
Pitts, J.R., Stanley, J.T., Fields, C.L., 1988. Solar induced surface transformation of materials (SISTM). In: Gupta, B.P., Traugott, W.H. (Eds.), Proceedings Fourth International Symposium on Solar Thermal Technology Santa Fe, N.M., June 13–17. Published by Hemisphere Publishing Corp., Washington D. C. (1990), pp. 459–470.
Rodriguez, G.P., López, V., Damborenea, J.J., Vázquez, A.J., 1995. Surface transformation hardening on steels treated with solar energy in a central tower and heliostats field. Solar Energy Mater. Solar Cells 37, 1–12.
Rodríguez, G.P., de Damborenea, J.J., Vázquez, A.J., 1997. Surface hardening of Steel in a solar furnace. Surf. Coatings Technol. 92, 165–170.
Rodríguez, G. P., García, I. and Vázquez, A. J., 1999, Coating processing by self-propagating high-temperature synthesis (SHS) using a Fresnel lens, J. de Physique IV France, Proceedings of the 9th Solar PACES International Symposium on Solar Thermal Concentrating Technologies, 9 (PR3), pp. 411–416.
Rodríguez, G.P., Herranz, G., Romero, A., 2013. Solar gas nitriding of Ti6Al4V alloy. Appl. Surf. Sci. 283, 445–452.
Romero, A., García, I., Arenas, M.A., López, V., Vázquez, A., 2013. High melting point metals welding by concentrated solar energy. Solar energy 95, 131–143.
Romero, A., García, I., Arenas, M.A., López, V., Vázquez, A., 2015. Ti_6Al_4V titanium alloy welded using concentrated solar energy. J. Mater. Process. Technol. 223, 284–291.
Sánchez-Bautista, C., Ferriere, A., Rodríguez, G.P., López-Almodovar, M., Barba, A., Sierra, C., Vázquez, A.J., 2006. NiAl intermetallic coatings elaborated by a solar assited SHS process. Intermetallics 14, 1270–1275.
Sánchez-Olías, J., García, I., Vázquez, A.J., 1999. Synthesis of TiN with solar energy concentrated by a Fresnel lens. Mater. Lett. 38, 379–385.
Sierra, C., Vázquez, A.J., 2005. NiAl coatings on carbon steel by self-propagating high-temperature synthesis assisted with concentrated solar energy: mass influence on adherence and porosity. Solar Energy Mater. Cells 86, 33–42.
Sierra, C., Vázquez, A.J., 2006. NiAl coating on carbon steel with an intermediate Ni gradient layer. Surf. Coatings Technol. 200, 4383–4388.
Stanley, J.T., Pitts, J.R., Fields, C.L., 1989. Solar induced surface transformation of steel samples. In: Yazici, R.M., Hoboken, N.J. (Ed.), Proceedings of the Fifth Annual Northeast Regional Meeting (TMS): Protective Coatings: Processing and Characterization Stevens Institute of Technology, May 3–5. Published by TMS, Warrendale, Pa. (1990), pp. 43–57.
Suresh, D., Rohatgi, P.K., 1979. Melting and casting of alloys in a solar furnace. Solar Energy 23, 553–555.
Suresh, D., Rohatgi, P.K., 1981. Heat transfer analysis on metal-melting in a foundry solar furnace. Solar Energy 26, 87–90.
Westwood, W. D., 1989, Physical Vapor Deposition, in Microelectronic Materials and Processes. In: Levy, R.A. (Ed.), NATO ASI Series (Series E: Applied Sciences). vol. 164, Dordrecht: Springer.
Yang, Y., Torrance, A.A., Rodríguez, J., 1996. The solar hardening of steels: Experiments and predictions. Solar Energy Mater. Solar Cells 40, 103–121.
Yu, Z.K., Zong, Q.Y., Tam, Z.T., 1982. A preliminary investigation on surface hardening of steel and iron by solar energy. J. Heat Treat. 2, 344–350.
Yu, Z.K., Lu, J.T., 1987. Microstructure and properties of nodular cast iron surface alloyed with tungsten carbide by concentrated solar energy. Surf. Eng. 3, 41–45.

References ceramics:

Adylov, G.T., Bibershtein, B.E., Voronov, G.V., Urazaeva, E.M., 1990. Alumina-magnesia spinel-based ceramic produced in a solar furnace. Refractories and Indus. Ceramics 31, 499–502.
Ashton Acton, Q., 2013, Eye Proteins- Advances in Research and Application, Atlanta, Georgia, USA: Scholarly Editions. p. 181.
Cardarelli, F., 2008, Materials Handbook. A Concise Desktop Reference, second edition, London, UK: Springer-Verlag, London Limited.
Ceballos-Mendivil, L.G., Cabanillas-López, R.E., Tánori-Córdova, J.C., Murrieta-Yesca, R., Pérez-Rábago, C.A., Villafrán-Vidales, H.I., Arancibia-Bulnes, C.A., Estrada, C.A., 2015. Synthesis of silicon carbide using concentrated solar energy. Solar Energy 116, 238–246.
Costa-Oliveira, F.A., Shohoji, N., Fernandes, J.C., Guerra-Rosa, L., 2005. Solar sintering of cordierite-based ceramics at low temperatures. Solar Energy 78, 351–361.
Costa-Oliveira, F.A., Cruz-Fernandes, J., Badie, J., Granier, B., Guerra-Rosa, L., Shohoji, N., 2007. High meta-stability of tungsten sub-carbide W_2C formed from tungsten/carbon powder mixture during eruptive heating in a solar furnace. Int. J. Refractory Metals Hard Mater. 25 (1), 101–106.
Costa-Oliveira, F.A., Granier, B., Badie, J.M., Cruz-Fernandes, J., Guerra-Rosa, L., Shohoji, N., 2008. Surface singularity upon solar radiation heating of graphite/tungsten powder mixture compacts to temperatures in excess of 1600°C. Mater. Sci. Forum 587–588, 993–997.
Costa-Oliveira, F.A., Rosa, L.G., Fernandes, J.C., Rodríguez, J., Cañadas, I., Martínez, D., Shojoji, N., 2009. Mechanical properties of dense cordierite discs sintered by solar radiation heating. Mater. Trans. 50, 2221–2228.
Costa-Oliveira, F.A., Guerra-Rosa, L., Peraudeau, G., Granier, B., Cruz-Fernandes, J., Magalhaes, T., Shohoji, N., 2012. Crystal grain morphology evolution over Ti, V, Nb and Ta Surface heated in N2 gas environment to 2000 °C by filtered concentrated solar beam in a solar furnace at PROMES-CNRS. Mater. Trans. 53 (3), 537–545.
Costa-Oliveira, F.A., Rosa, L.G., Fernandes, J.C., Rodríguez, J., Cañadas, I., Magalhaes, T., Shohoji, N., 2015. Nitriding VI-group metals (Cr, Mo and W) in stream of NH_3 gas under concentrated solar irradiation in a solar furnace at PSA (Plataforma Solar de Almería). Solar Energy 114, 51–60.
Costa-Oliveira, F.A., Figueira-Vasques, I., Cruz-Fernandes, J., Cañadas, I., Rodríguez, J., Guerra-Rosa, L., Shohoji, N., 2016. Reactions of IVa-group metals, Ti and Zr, with uncracked NH3 gas at a temperature in the range between 600 and 800 °C under heating with concentrated solar beam at PSA. Solar Energy 138, 119–127.
Cruz-Fernandes, J., Guerra, L., Martínez, D., Rodríguez, J., Shohoji, N., 1998. Influence of gas environment on synthesis of silicon carbide through reaction between silicon and amorphous carbon in a solar furnace at PSA (Plataforma Solar de Almería). J. Ceramic Soc. Japan 106, 839–841.
Cruz-Fernandes, J., Amaral, P.M., Guerra-Rosa, L., Martínez, D., Rodríguez, J., Shohoji, N., 1999. X-ray diffraction characterization of carbide and carbonitride of Ti and Zr prepared through reaction between metal powders and carbon powders (graphitic or amorphous) in a solar furnace. Int. J. Refractory Metals Hard Mater. 17, 437–443.
Cruz-Fernandes, J., Amaral, P.M., Guerra-Rosa, L., Shohoji, N., 2000. Weibull statistical analysis of flexure breaking performance for alumina ceramic disks sintered by solar radiation heating. Ceramics Int. 26, 203–206.
Cruz-Fernandes, J., Anjinho, C., Amaral, P.M., Guerra-Rosa, L., Rodríguez, J., Martínez, D., Almeida Costa Oliveira, F., Shohoji, N., 2002. Characterization of solar-synthesised TiC_X (X = 0.5, 0.625, 0.75, 0.85, 0.90 and 1.0) by x-ray diffraction, density and Vickers microhardness. Mater. Chem. Phys. 77, 711–718.
Cruz-Fernandes, J., Costa-Oliveira, F.A., Granier, B., Badie, J., Guerra-Rosa, L., Shohoji, N., 2006. Kinetic aspects of reaction between tantalum and carbon material (active carbon or graphite) under solar radiation heating. Solar Energy 80, 1553–1560.
Dias, S., Costa-Oliveira, F.A., Granier, B., Badie, J., Cruz-Fernandes, J., Guerra-Rosa, L., Shohoji, N., 2007. Nano-meter size WC whiskers grown over a compacted pellet of graphite/tungsten powder mixture heated with an ultra-fast heating rate by a concentrated solar beam. Mater. Trans. 48 (5), 919–923.
Fernandes, J.C., Oliveira, F.A.C., Rosa, L.G., Rodríguez, J., Cañadas, I., Magalhaes, T., Shohoji, N., 2016. Low-temperature short-time nitriding of Va-group metals, V, Nb and Ta, in uncracked NH_3 gas under heating with concentrated solar power (CSP). Ciência Tecnologia dos Materiais 28 (2), 112–116.
Granier, B., Badie, J., Costa-Oliveira, F.A., Magalhaes, T., Shohoji, N., Guerra-Rosa, L., Cruz-Fernandes, J., 2008. Carbide synthesis from graphite/molybdenum powder mixtures at sub-stoichiometric ratios under solar radiation heating to 1900 °C. Mater. Trans. 49 (11), 2673–2678.
Granier, B., Shohoji, N., Costa-Oliveira, F.A., Magalhaes, T., Cruz-Fernandes, J., Guerra-Rosa, L., 2009. Carbide phases synthesised from C/Mo powder compacts at specified sub-stoichiometric ratios by solar radiation heating to temperatures between 1600 °C and 2500 °C. Mater. Trans. 50 (12), 2813–2819.
Guerra-Rosa, L., Cruz-Fernandes, J., Amaral, P.M., Martínez, D., Rodríguez, J., Shohoji, N., 1999. Photochemically promoted formation of higher carbide of molybdenum through reaction between metallic molybdenum powders and graphite powders in a solar furnace. Int. J. Refractory Metals Hard Mater. 17 (5), 351–356.
Guerra-Rosa, L., Miguel-Amaral, P., Anjinho, C., Cruz-Fernandes, C., Shohoji, N., 2002. Fracture toughness of solar-sintered WC with Co additive. Ceramics Int. 28, 345–348.
Gulamova, D.D., Uskenbaev, D.E., Turdiev, Zh. Sh., Toshmurodov, Yo.K., Bobokulov, S. H., 2009, Synthesis of silicon carbide by exposure to solar radiation, Appl. Solar Energy, 45, pp. 105–108.
Hench, L.L., West, J.K., 1990. The sol-gel process. Chem. Rev. 90 (1), 33–72.
Lightstone, J.M., Mann, H.A., Wu, M., Johnson, P.M., White, M.G., 2003. Gas-phase production of molybdenum carbide, nitride, and sulfide clusters and nanocrystallites. J. Phys. Chem. B 107 (38), 10359–10366.

Ma, Y., Guan, G., Hao, X., Cao, J., Abudula, A., 2017. Molybdenum carbide as alternative catalyst for hydrogen production- A review. Renew. Sustain. Energy Rev. 75, 1101–1129.
Martínez, D., Rodríguez, J., Guerra-Rosa, L., Cruz-Fernandes, J., Shohoji, N., 1999. Influence of gas environment on synthesis of silicon carbide and some carbides and carbonitrides of d-group transition metals through reaction between metal powders and amorphous carbon powders in a solar furnace at PSA (Plataforma Solar de Almería). J. Phys. IV France 09, 405–410.
Murray, J.P., Steinfeld, A., Fletcher, A., 1995. Metals, nitrides and carbides via solar carbothermal reduction of metal oxides. Energy 20, 695–704.
Nagai, M., Shishikura, I., Omi, S., 2000. Molybdenum carbide prepared by chemical vapor deposition. Japanese J. Appl. Phys. 39, 4528–4531.
Paizullakhanov, M.S., Faiziev, Sh.A., 2006. Calcium carbide synthesis using a solar furnace. Tech. Phys. Lett. 32 (3), 211–212.
Pero-Sanz, J.A., Quintana, M.J., Verdeja, L.F., 2017. Solidification and Solid-State Transformations of Metals and Alloys, first ed. Elsevier Inc, Boston, USA.
Rodríguez, J., Martínez, D., Guerra-Rosa, L., Cruz-Fernandes, Amaral, P.M., Shohoji, N., 2001. Photochemical effects in carbide synthesis of d-group transition metals (Ti, Zr; V, Nb, Ta; Cr, Mo, W) in a solar furnace at PSA (Plataforma Solar de Almería). J. Solar Energy Eng. 123 (2), 109–116.
Román, R., Cañadas, I., Rodríguez, J., Hernández, M.T., González, M., 2008. Solar sintering of alumina ceramics: microstructural development. Solar Energy 82, 893–902.
Shohoji, N., Guerra-Rosa, L., Cruz-Fernandes, J., Martínez, D., Rodríguez, J., 1999. Catalytic acceleration of graphitisation of amorphous carbon during synthesis of tungsten carbide from tungsten and excess amorphous carbon in a solar furnace. Mater. Chem. Phys. 58 (2), 172–176.
Shohoji, N., Amaral, P.M., Cruz-Fernandes, J., Guerra-Rosa, L., Martínez, D., Rodríguez, J., 2000. Catalytic graphitization of amorphous carbon during solar carbide synthesis of VI a group metals (Cr, Mo, and W). Mater. Trans. 41, 246–249.
Shohoji, N., Badie, J., Granier, B., Costa-Oliveira, F.A., Cruz-Fernandes, J., Guerra-Rosa, L., 2007. Formation of hexagonal η-MoC1-x phase at a temperature lower than 1660 °C by solar radiation heating under presence of excess free carbon. Int. J. Refractory Metals Hard Mater. 25 (3), 220–225.
Shohoji, N., Magalhaes, T., Costa-Oliveira, F.A., Guerra-Rosa, L., Cruz-Fernandes, J., Rodríguez, J., Cañadas, I., Martínez, 2010. Heterogeneity along the height in disc specimens of graphite/tungsten powder mixtures with sub-stoichiometric carbon atom ratios heated by concentrated solar beam to 1600 °C. Mater. Trans. 51 (2), 381–388.
Shohoji, N., Costa-Oliveira, F.A., Guerra-Rosa, L., Peraudeau, G., Granier, B., Magalhaes, T., Cruz-Fernandes, J., 2011. Reactions of Ti, V, Nb and Ta with N_2 gas at 2000°C under concentrated solar beam in a solar furnace at PROMES-CNRS. Mater. Trans. 52 (4), 719–727.
Shohoji, N., Costa-Oliveira, F.A., Guerra-Rosa, L., Cruz-Fernandes, J., Magalhaes, T., Caldeira-Coelho, M., Rodríguez, J., Cañadas, I., Ramos, C., Martínez, D., 2012. Synthesising carbo-nitrides of some d-group transition metals using a solar furnace at PSA. Mater. Sci. Forum 730–732, 153–158.
Shohoji, N., Costa-Oliveira, F.A., Fernandes, J.C., Guerra-Rosa, L., Rodríguez, J., Cañadas, I., Ramos, C., Magalhaes, T., Cestari, F., 2013. Synthesizing higher nitride of molybdenum (Mo) and iron (Fe) in amonia (NH_3) gas stream under irradiation of concentrated solar beam in a solar furnace. Materialwissenschaft und Werkstofftechnik 44, 959–971.
Verdeja, L. F., Sancho, J. P., Ballester, A. and González, R., 2014. Refractory and Ceramic Materials, Madrid: Ed. Síntesis.
Wang, H., Wang, X., Zhang, M., Du, X., Li, W., Tao, K., 2007. Synthesis of bulk and supported molybdenum carbide by a single-step thermal carburization method. Chem. Mater. 19, 1801–1807.
Wang, Y., Tu, W., Hong, J., Zhang, W., Xu, R., 2016. Molybdenum carbide microcrystals: Efficient and stable catalyst for photocatalytic H_2 evolution from water in presence of dye sensitizer. J. Materiomics 2 (44), 344–349.
Zhilinska, N., Zalite, I., Rodríguez, J., Martínez, D., Cañadas, I., 2003. "Sintering of nanodisperse powders in a solar furnace", EUROPM2003. Sintering 423–428.

References fullerenes and carbon nanotubes:

Amer, M.S., 2010. Raman Spectroscopy, Fullerenes and Nanotechnology. Royal Society of Chemistry Publishing, Cambridge, UK.
Chibante, L.P.F., Thess, A., Alford, J.M., Diener, M.D., Smalley, R.E., 1993. Solar generation of the fullerenes. J. Phys. Chem. 97, 8696–8700.
De Volder, M.F.L., Tawfick, S.H., Baughman, R.H., Hart, A.J., 2013. Carbon nanotubes: Present and future commercial applications. Science 339 (6119), 535–539.
Fields, C.L., Pitts, J.R., Hale, M.J., Bingham, C., Lewandowski, A., King, D.E., 1993. Formation of fullerenes in highly concentrated solar flux. J. Phys. Chem. 97, 8701–8702.
Flamant, G., Luxembourg, D., Robert, J.F., Laplaze, D., 2004a. Optimizing fullerene synthesis in a 50kW solar reactor. Solar Energy 77, 73–80.
Flamant, G., Robert, J.F., Marty, S., Gineste, J.M., Giral, J., Rivoire, B., Laplaze, D., 2004b. Solar reactor scaling up: the fullerene synthesis case study. Energy 29, 801–809.
Flamant, G., Bijeire, M., Luxembourg, D., 2005. Modelling of a solar reactor for single-wall nanotube synthesis. J. Solar Energy Eng. 128 (1), 24–29.
Guillard, T., Flamant, G., Laplaze, D., 2001a. Heat, mass, and fluid flow in a solar reactor for fullerene synthesis. J. Solar Energy Eng. 123 (2), 153–159.
Guillard, T., Flamant, G., Robert, J., Rivoire, B., Giral, J., Laplaze, D., 2001b. Scale up of a solar reactor for fullerene and nanotube synthesis. J. Solar Energy Eng. 124 (1), 22–27.
Hale, M. J., Fields, C., Lewandowski, A., Bingham, C. and Pitts, R., 1994, Production of fullerenes with concentrated flux, ASME/JSME/JSES International Solar Energy Conference, San Francisco, California, March 27–30, pp. 1–9.
Laplaze, D., Bernier, P., Flamant, G., Lebrun, M., Brunelle, A., Della-Negra, S., 1996. Solar energy: Application to the production of fullerenes. J. Phys. B. 29, 4943–4954.
Luxembourg, D., Flamant, G., Laplaze, D., 2005. Solar synthesis of single-walled carbon nanotubes at medium scale. Carbon 43, 2302–2310.

References lime production:

Flamant, G., Hernandez, D., Traverse, J., 1980. Experimental aspects of the thermochemical conversion of solar energy; Decarbonation of $CaCO_3$. Solar energy 24 (4), 385–395.
Imhof, A., 1997. Decomposition of limestone in a solar reactor. Renew. Energy 10 (2/3), 239–246.
Meier, A., Bonaldi, E., Cella, G.M., Lipinski, W., Wuillemin, D., Palumbo, R., 2004. Design and experimental investigation of a horizontal rotary reactor for the solar thermal production of lime. Energy 29, 811–821.
Meier, A., Bonaldi, E., Cella, G.M., Lipinski, W., 2005a. Multitube rotary kiln for the industrial solar production of lime. J. Solar Energy Eng. 127 (3), 386–395.
Meier, A., Gremaud, N., Steinfeld, A., 2005b. Economic evaluation of the industrial solar production of lime. Energy Conver. Manage. 46, 905–926.
Meier, A., Bonaldi, E., Cella, G.M., Lipinski, W., Wuillemin, D., 2006. Solar chemical reactor technology for industrial production of lime. Solar Energy 80, 1355–1362.
Salman, O.A., 1988. Thermal decomposition of limestone and gypsum by solar energy. Solar energy 41 (4), 305–308.